NeuroImage 195 (2019) 89–103

Contents lists available at ScienceDirect

NeuroImage

journal homepage: www.elsevier.com/locate/neuroimage

Anesthesia differentially modulates neuronal and vascular contributions to the BOLD signal

Timo Mauritz van Alst [a], Lydia Wachsmuth [a], Maia Datunashvili [b], Franziska Albers [a], Nathalie Just [a], Thomas Budde [b], Cornelius Faber [a,*]

[a] Department of Clinical Radiology, Translational Research Imaging Center (TRIC), University Hospital Münster, Germany
[b] Institute of Physiology I, Westfälische Wilhelms University Münster, Germany

ARTICLE INFO

Keywords:
fMRI
Carbon dioxide
Fiber-based calcium recordings
Neural activity
Perfusion
Isoflurane

ABSTRACT

Most studies involving BOLD fMRI in basic neuroscience research are conducted with anesthetized animals. This study investigates neural and hemodynamic activity through a combination of experiments comprising BOLD fMRI, optical calcium recordings and ASL in vivo. Patch clamp experiments of neurons were conducted to evaluate electrophysiological correlates of neural activity in vitro. Various anesthetic conditions embracing numerous anesthetic depths evoked by different concentrations of isoflurane (ISO) and different degrees of hypercapnia under a constant stimulus were investigated. We observed that different anesthetic conditions had major impact on the results obtained, particularly that anesthesia could cause a massive divergence of different experimental modalities.

In ventilated animals, robust BOLD responses were detectable even with relatively deep anesthesia, while in non-ventilated animals, BOLD responses were not detectable under these conditions. This was most likely due to hypercapnia caused by respiratory depression, as in ventilated animals administered CO_2 had the same effect. This observation agreed with measurements of perfusion, which showed that inhaled CO_2 increased perfusion significantly, while ISO did not.

In optical calcium measurements, higher concentrations of ISO decreased spontaneous neural activity, but not stimulus-evoked responses. This observation was explained by a generally lower excitability of neurons under ISO, which suppressed spontaneous activity, and consequently left more neurons available to fire synchronously in response to a stimulus. Interpreting this phenomenon as an integrated signal of independent single neurons was supported by patch clamp experiments as the number of action potentials (APs) per stimulus was decreased by addition of CO_2. Addition of ISO on the other hand had no significant effect.

Our results provide an explanation on the cellular level for anesthesia-dependent observations in previous studies of task-induced BOLD and resting state connectivity. They further inform selection of the adequate anesthetic regimen for a given combination of modalities.

1. Introduction

BOLD fMRI provides a tool for detection and mapping of brain activation. BOLD responses do not directly reflect neural activity though, but rather alterations in cerebral hemodynamics indirectly caused by neural activity. BOLD is thus not linearly dependent on neural activity, but is affected by intravascular magnetic susceptibility, cerebral blood volume (CBV), cerebral blood flow (CBF), cerebral metabolic rate of oxygen ($CMRO_2$) and particularly the neurovascular coupling (Hillman, 2014) as an overarching concept of the parameters connecting neural activity and BOLD. Despite extensive research for almost 30 years, the exact relation between BOLD and underlying neural activity remains unclear (Ekstrom, 2010; Heeger and Ress, 2002; Logothetis et al., 2001). Although this is a well-recognized fact, its practical consequences are often ignored (Logothetis, 2008).

fMRI in preclinical and basic neuroscience research is mainly conducted with anesthetized animals, especially with rodents. Anesthesia is known to alter both neural activity and hemodynamic state. The extent of alteration varies and is, at least in part, not known (Aksenov et al., 2015; Berwick et al., 2002; Martin et al., 2006; Williams et al., 2010). In studies

* Corresponding author. Albert-Schweitzer-Campus 1, Building A16, 48149, Münster, Germany.
E-mail address: faberc@uni-muenster.de (C. Faber).

https://doi.org/10.1016/j.neuroimage.2019.03.057
Received 6 November 2018; Received in revised form 6 March 2019; Accepted 25 March 2019
Available online 28 March 2019

involving fMRI, it is therefore crucial to ask which of the observed effects originate from the individual regressor itself and which from anesthesia – most importantly because anesthetics can be responsible for an uncoupling between neural activity and BOLD signal.

Performing fMRI experiments in awake animals avoids unknown effects from anesthetics (Gao et al., 2017). However, issues like acute and long-term changes in physiology or artificial responses due to restraint and stress remain an issue (Low et al., 2016). Therefore, a broad range of anesthetics is still used, e.g. alpha-chloralose, urethane, propofol and volatile anesthetics such as isoflurane (ISO) and sevoflurane. Each anesthetic alters brain functionality and connectivity through different pharmacological pathways, which have different impact on neural and vascular response and the neurovascular coupling (Masamoto and Kanno, 2012). For fMRI, in particular for longitudinal studies, medetomidine (MED) and ISO are frequently used. The combination of MED and ISO (Brynildsen et al., 2017; Fukuda et al., 2013; Grandjean et al., 2014; Zhao et al., 2012) provides more stable physiological conditions than constant MED infusion alone (Fukuda et al., 2013; Pawela et al., 2009; Sommers et al., 2002; Weber et al., 2006; Zhao et al., 2008). The exact effects of anesthetics on individual components of the neurovascular unit, however, remain largely unclear.

Compared to BOLD fMRI, calcium recordings provide a more direct readout of neural activity. A combination of both is suitable to separate neural from vascular responses, and furthermore less prone to artefacts as compared to the combination of fMRI and electrical recordings. Hence, parallel acquisition of fMRI and calcium recordings has been implemented and is increasingly used (Liang et al., 2017; Schlegel et al., 2018; Schmid et al., 2016; Schulz et al., 2012; Schwalm et al., 2017).

In the present study, we aimed to investigate how various conditions, including different depths of anesthesia and various physiological conditions affect BOLD and underlying parameters like perfusion and neural activity. As BOLD signals represent complex quantities, we established a combination of experiments to characterize different aspects of neural activity that play a role in the BOLD signal. We recorded BOLD and simultaneously performed calcium recordings to assess task-related and spontaneous neural activity in vivo, Arterial Spin Labeling (ASL) to assess perfusion and in vitro patch clamp experiments to determine cellular properties without spontaneous activity. We wanted to assess whether, and if so, how neural activity in BOLD fMRI and underlying parameters can be dissociated. In a first step we used non-ventilated animals. Different depths of anesthesia were achieved with a constant MED infusion and a varying dose of ISO while a constant electrical stimulus was applied. In a second step, ventilated animals were subjected to the same experimental conditions. Additionally, we administered CO_2 in some experiments.

2. Material and methods

All experiments were performed according to the German Tierschutzgesetz and were approved by local authorities (Landesamt für Natur, Umwelt und Verbraucherschutz Nordrhein-Westfalen, Germany [approval ID 84–02.04.2015.A427 and 84–02.04.2014.A347 for in vivo experiments; 84–02.05.50.15.026 for in vitro/patch clamp experiments]). Rats were obtained from Charles River, Sulzfeld, Germany, were housed in groups of 2–3, were kept at a 12/12 h light/dark cycle and had free access to water and standard diet. Animals weighed 201 ± 52 g.

To discriminate between effects coming from hypoventilation under deep anesthesia and direct effects of anesthetics, two groups of animals were formed, spontaneously breathing animals and ventilated animals.

A total number of 14 spontaneously breathing female Fischer rats was investigated by fMRI, 7 of these obtained simultaneous calcium recordings, 6 were subject to ASL MRI to assess cerebral perfusion. To assess possible differences between rat strains, 10 spontaneously breathing SD rats (5 male, 5 female) were subject to fMRI only.

fMRI procedures were also conducted in 13 ventilated Fischer rats, 6 of these additionally obtained simultaneous calcium recordings. 6 ventilated Fischer rats were subject to ASL fMRI.

For a detailed overview of animals for in vivo experiments, see Suppl. Table 1. Fig. 1 gives an overview of in vivo experiments and sequential arrangement for a rat undergoing BOLD fMRI and simultaneous calcium recordings as well as ASL. Note that not all animals were subject to all experimental conditions of this study.

2.1. Animal preparation and BOLD fMRI

Anesthesia induction was performed by placing the rat in a gas anesthesia box using oxygen enriched with 5% ISO (Forene, Abbott, Wiesbaden, Germany). Afterwards, the animal was mounted on a heated MRI cradle, fixed via bite- and ear bars and supplied with a mixture of 80% air and 20% oxygen enriched with ISO. Electrodes were subcutaneously inserted into one forepaw and connected to an electrical stimulator (DS5, Digitimer, Welwyn Garden City, UK). The animals were transferred to a 9.4 T small animal MRI with a 0.7 T/m gradient system (Biospec 94/20, Bruker Biospin GmbH, Ettlingen, Germany) with a 20-mm surface coil for detection and a 72-mm transmit volume coil.

MED (Orion Corporation, Espoo, Finland) infusion was started (40 µg/kg bolus, followed by infusion of 50 µg/kg/h) and ISO was discontinued. Measurements began 40 min after start of MED infusion.

The forepaw was electrically stimulated (5 s stimulation [9 Hz, 1 mA, 1 ms pulse width], 25 s rest), repeatedly for 600 s fMRI BOLD was

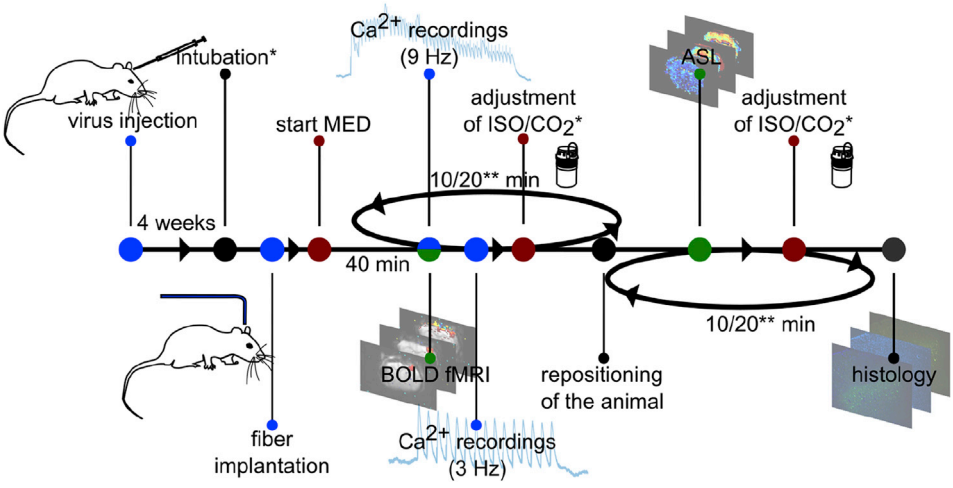

Fig. 1. Overview of in vivo experiments. *intubation was only conducted for ventilated animals. Spontaneously breathing animals were not intubated. **10 min waiting time after ISO was adjusted with a difference of max. 0.3% ISO. For higher differences and for measurements with CO_2, 20 min waiting time was allowed.

performed using a single-shot GE-EPI (TR = 1 s, TE = 18 ms, 600 repetitions, resolution 0.325 × 0.35 mm^2, 9 contiguous slices, slice thickness 1.2 mm).

In spontaneously breathing animals, stimulation experiments were performed under stepwise increased and later decreased ISO concentrations (seven steps: 0.0%, 0.2%, 0.4%, 0.7%, 1.0%, 1.25%, 1.5%) so that the first and last measurement were conducted under pure MED sedation without ISO. fMRI was repeated for each step using the same stimulation paradigm, and allowing 10 min equilibration time after concentration had been adjusted. Where possible, two measurements per animal were taken. If the respiratory rate (RR) was more than 85/min, anesthesia was deepened, if RR went below 20/min, anesthesia was reduced. In both cases, respective measurements were interrupted, and data was discarded. Respiratory rate and rectal temperature were continuously monitored for all animals.

Ventilated animals were intubated before placing the rat on the MRI cradle. The valve was connected to a ventilator (MRI-1 Ventilator, CWE Inc., Ardmore, PA, USA). The expiration tube was coupled with a CO_2 analyzer (CapStar-100 CO_2 Analyzer, CWE Inc., Ardmore, PA, USA). Ventilation settings were adjusted for each animal, so that the CO_2 concentration in the expiratory flow was in a narrow range around 3% CO_2. Ventilated animals were paralyzed through intravenous application of Pancuronium (2 mg/kg bolus, 1.5 mg/kg continuous infusion; Pancuronium Inresa, Inresa Arzneimittel GmbH, Freiburg, Germany).

For ventilated animals, the number of different ISO concentrations was reduced to four steps (0.0%, 0.2%, 0.7%, 1.5%). We additionally combined 0.0% and 1.5% ISO with 5% CO_2 in the inspiratory air. The number of steps of different ISO concentrations was reduced to keep the experiments in an acceptable time frame. If the dose increment was more than 0.3% ISO or if CO_2 was added, the waiting time was increased to 20 min before the measurement was started. Average time between anesthesia induction and data acquisition was 131 min.

fMRI analysis was performed with SPM8 (Wellcome Trust Centre for Neuroimaging, Institute of Neurology, UCL, London, UK). To reduce signal variation, the first five scans were discarded from each imaging series. Data were motion-corrected and smoothed with a gaussian kernel of 0.5 mm. For an initial graphical representation of the activation maps, a hemodynamic response function designed for the temporal characteristics of BOLD in rats was used in order to model the BOLD response to electrical stimulation. The data were corrected for multiple comparisons (family wise error correction) and statistical significance was set at $p < 0.05$. The mean EPI image was overlayed with resulting t-score maps. A ROI (3x3 Voxels) was defined within the activated area of the somatosensory cortex of the forepaw (S1Fl). The ROI was placed at the maximum signal intensity at 0.2% ISO. If no voxels were marked as activated, the ROI was drawn in the centre of S1Fl. Using custom-written MATLAB (The MathWorks, Inc., Natick, Massachusetts, USA) scripts, BOLD intensities of this ROI were summed over all stimulations of one experiment and extracted. Time courses for matching conditions were averaged (Fig. 2a–f).

2.2. Stereotactic injections and calcium recordings

For calcium recordings, rats were virally transduced with the genetically encoded calcium indicator (GCaMP6f) under control of either Synapsin or calmodulin-dependent protein kinase II (CamKII) promotor. Viral constructs were obtained from GENIE project, Janelia Research Campus, Howard Hughes Medical Institute (Vivek Jayaraman, Douglas S. Kim, Loren L. Looger, Karel Svoboda). Anesthesia induction was performed as stated above (2.1). Additionally, animals were treated with Buprenorphin (Indivior UK Ltd, UK) s.c. (0.05 mg/kg). Lidocain (AstraZeneca AB, Södertälje, Sweden) was locally applied. Rats were placed on a warming pad. The head was fixed using a stereotactic frame via bite bar and ear plugs. Stereotactic injections were executed under 1.5–2.8% ISO. A craniotomy was made using a dental drill (Ultimate XL-F, NSK, Trier Germany). Drilling and injection were performed using a 34° angle from medial (relative to the bregma: anterior-posterior [AP]: 0.2 mm, left-right [LR]: 2.4 mm, dorso-ventral [DV] 1.6 mm) according to stereotactic coordinates (Paxinos and Watson, 1997) and corresponding to the localization of S1Fl.

1 µl of adeno-associated virus particles (AAV1) containing CamKII.GCaMP6f.WPRE.SV40 was injected in 4 rats for experiments with spontaneous breathing, and in 4 rats for experiments with ventilation. 3 rats for experiments with spontaneous breathing and 2 rats for experiments with ventilation received AAV1 containing Syn.GCaMP6f.WPRE.SV40. Injection was performed in S1Fl with a syringe pump (World Precision Instruments, Sarasota, FL, USA) at a speed of 0.5 µl/min. After injection, the capillary was held in position for 5 min before it was slowly retrieved. The scalp was closed with a suture. Acute experiments were conducted 4 weeks after injection at the earliest to maximize expression of GCaMP (Akerboom et al., 2012).

For the acute experiments, in order to avoid reopening of the bore, an optic fiber (diameter 200 µm) was implanted straightly in S1FL (AP: 0.2 mm, LR 3.3 mm, DV 0.2–0.3 mm (Paxinos and Watson, 1997), and was connected to a blue laser (488 nm, Sapphire, Coherent, Dieburg, Germany) delivering excitation light. Using the same fiber, fluorescent light was detected. The measured level of fluorescence was dependent on intracellular binding of calcium ions to GCaMP. Since calcium influx is related to electrical activity, it was possible to detect neural activity. For a detailed description, see Albers et al. (2018) and Schmid et al. (2016).

MED infusion was started and ISO was discontinued. The animal was transferred to the MRI for simultaneous BOLD + calcium recordings. Anesthesia, stimulation and fMRI stayed the same as in sole fMRI BOLD measurements (see 2.1). Additionally to 9 Hz stimulation, we recorded calcium responses to 3 Hz stimulation (1 mA, 1 ms (pulse width), 5 s stim. + 25 s rest) for 300 s for each ISO concentration.

The calcium signal was reported as relative change of fluorescence to baseline (Δf/f). The average stimulation train was calculated for each trace as the mean of 20 (9 Hz stimulation) or 10 (3 Hz stimulation) stimulation periods. There were at maximum two traces per anesthetic condition per animal. For each anesthetic condition, all corresponding traces were considered (examples of calcium traces are shown in Fig. 3a–f) and mean ± SD of fluorescence was calculated (Fig. 4).

The fast kinetics of GCaMP6f enabled us to resolve single, individual responses (Fig. 3g and h). We analyzed the mean of primary responses over the whole stimulation period and whether the primary responses adapted over time.

Spontaneously breathing animals receiving Syn.GCaMP6f and CamKII.GCaMP6f both showed lower amplitudes when ISO was added to the inspiratory and were treated as one.

For comparison of amplitudes of the calcium signal between different inspiratory conditions, we took the mean of all amplitudes recorded during one stimulation period, and normalized it to the respective recordings under pure MED sedation. Amplitudes occurring for other inspiratory conditions within the same animal were reported relative to this value.

Especially for stimulation with 9 Hz, the fluorescence signal did not return to its initial value between two pulses (Fig. 3h, blue line). We therefore calculated the fluorescence amplitude as difference to a linear interpolation of the level of fluorescence at the beginning of each stimulation pulse (Fig. 3h, red line). After subtracting this interpolated level of fluorescence, the amplitude of fluorescence change after each stimulation pulse was obtained (Fig. 5b, d, f, h, j, l).

To analyze whether the adaptation over the time course of 5 s was altered for different anesthetic conditions, we applied a different kind of normalization than stated above. In one stimulation period of 5 s, there were either 15 (for 3 Hz) or 45 (for 9 Hz) pulses and as a consequence up to 15 or up to 45 neuronal responses in the calcium signal. The change of fluorescence (Δf/f) for each neuronal response was normalized to the neuronal response with the highest amplitude within one stimulation period.

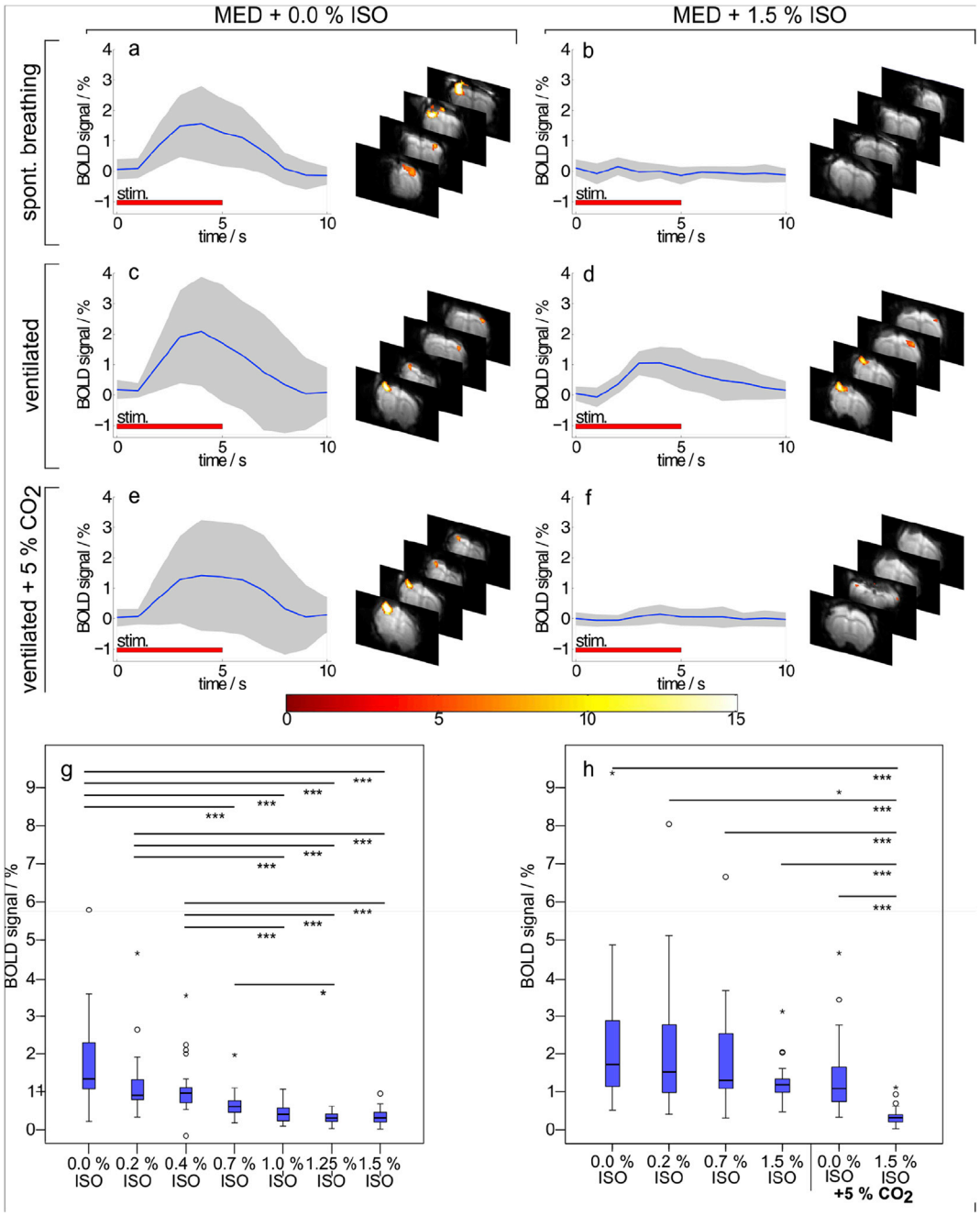

Fig. 2. Average BOLD timecourses and t-maps for given anesthetic parameters. Timecourses of 10 s are displayed, red line indicates forepaw stimulation with 9 Hz. BOLD timecourses are shown as the average (blue line) with standard deviation (gray shading) of all animals. Color bar indicates the t-value. (**a-b):** Animals were spontaneously breathing 80/20 air/oxygen with 0.0 %–1.5% ISO in the inspiratory air. (**c-d)**: Animals being ventilated with 80/20 air/oxygen with 0.0 %–1.5% ISO. (**e-f**): Animals being ventilated with the same air/oxygen mixture enriched with 5% CO_2. (**g**): BOLD amplitudes of spontaneously breathing animals. (**h**): BOLD amplitudes of ventilated animals.
Boxplots represent data between first and third quartiles, the band in the box marks the second quartile (=median). Whiskers represent lowest and highest data within 1.5 interquartile ranges (IQR) of the lower and upper quartile. Outliers within 1.5 and 3 IQR are marked as dots, values outlying 3 IQR are marked stars. * ≙ $p < 0.05$; ** ≙ $p < 0.01$; *** ≙ $p < 0.001$.

After completion of measurements, animals subject to calcium recordings were perfused transcardially with 4% paraformaldehyde. Brains were excised and transferred to paraformaldehyde solution for overnight fixation. Brains were then transferred to 30% sucrose solution. Using a vibratome (Leica, Wetzlar, Germany), coronal slices (20 μm) were prepared and stained with DAPI. Microscopy was performed on a fluorescence microscope (Nikon Eclipse 50i, Nikon Corporation, Tokyo, Japan) to validate GCaMP expression (Suppl. Fig. 1).

2.3. ASL

To quantify baseline perfusion under various anesthetic depths, we used a single-slice FAIR (flow-sensitive alternating inversion recovery) RARE (rapid acquisition with relaxation enhancement) protocol (TR = 18000 ms, TE = 25.55 ms, slice thickness 1.2 mm, matrix 128x64), with interleaved selective inversion and global inversion, a hyperbolic secant adiabatic pulse (pulse duration of 20 ms and bandwidth of 5 kHz) and 19 inversion times (minimum 30 ms, maximum 11000 ms).

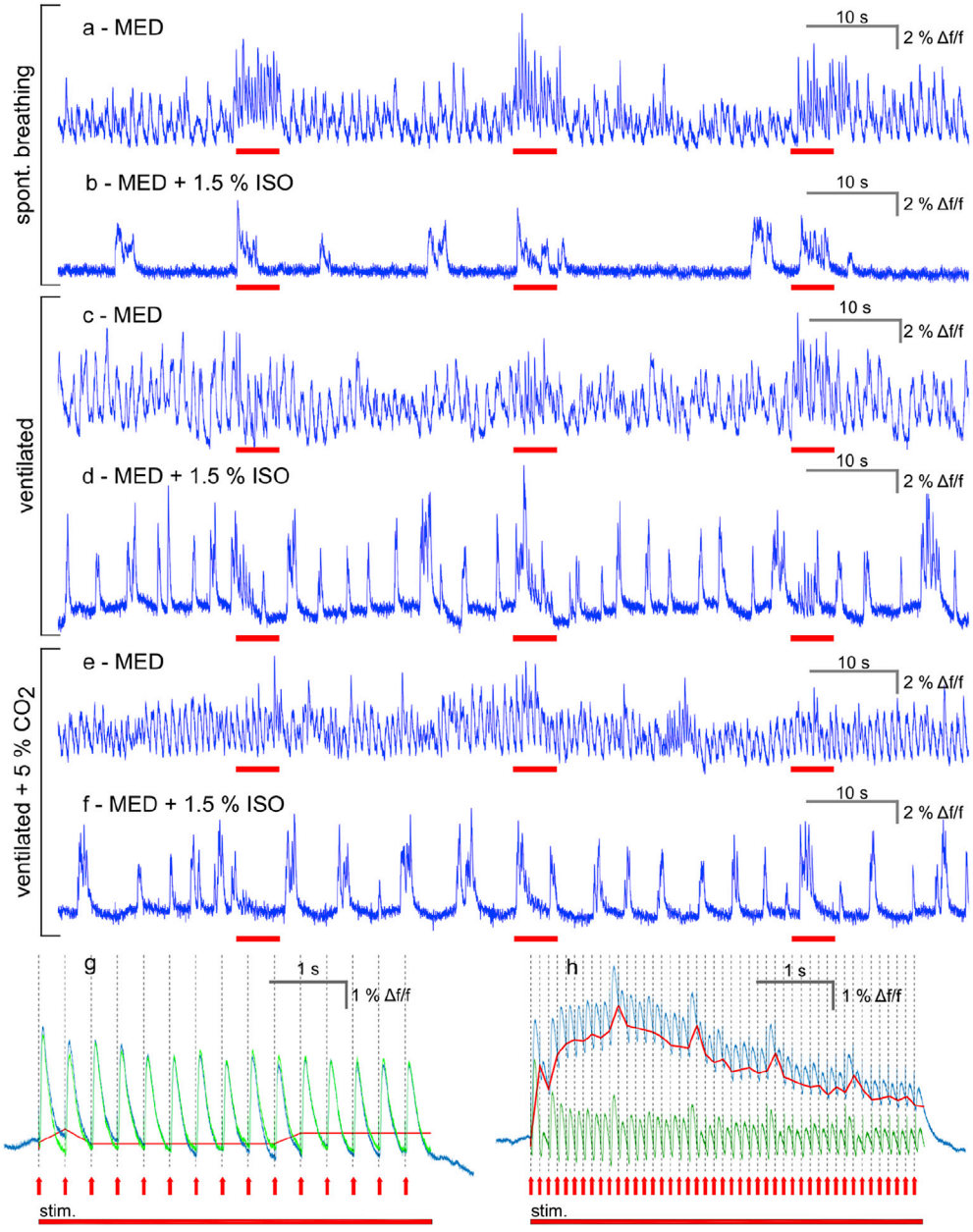

Fig. 3. Selection of Calcium traces. (**a-f**): selection of calcium traces under different anesthetic conditions. 5 s of stimulation (red boxes) with 3 Hz alternating with 25 s of rest. (**g,h**): averaged timecourse (blue) for 3 Hz (**g**) and 9 Hz stimulation (**h**) in spontaneously breathing animals at 0.0% ISO. The level of fluorescence at the beginning of each stimulation pulse was determined and these points were linearly interpolated (red graph). This level of fluorescence was subtracted from the averaged timecourse to analyze the shape of primary responses (green line).

In order to increase perfusion signal, care was taken during positioning of the animal to ensure coverage of heart and liver by the volume coil (Nasrallah et al., 2012). After BOLD fMRI, we therefore repositioned the animal before ASL was started (Fig. 1).

For perfusion experiments, T1 maps were calculated with MATLAB as described previously (Driencourt et al., 2017). A ROI was drawn in the S1Fl and perfusion values were extracted. The ROI was placed in the same slice as ROI of fMRI analysis and was drawn by hand to reflect only the cortex, resulting in a total number of voxels of 175 ± 2. Voxels with values above 400 ml/100 g/min were regarded to be blood vessels and excluded from analysis, as were voxels with values under 30 ml/100 g/min.

There were two values for each inspiratory condition per animal – measurements at 0.0% ISO were conducted at the very beginning and the very end of each series of measurements. To assess the alteration of perfusion for each animal relative to light sedation, absolute perfusion values were normalized to the last measurement at 0.0% ISO for each animal.

2.4. Patch clamp recordings

Patch clamp experiments were done on Fischer rats ranging in age from postnatal day P40-60. Rats were sacrificed, a skull cap caudal to the bregma was surgically removed and the brain tissue containing somatosensory cortex was submerged in ice-cold aerated (O_2) saline containing (in mM): sucrose (200), PIPES (20), KCl (2.5), NaH_2PO_4 (1.25), $MgSO_4$ (10), $CaCl_2$ (0.5), dextrose (10), pH = 7.34, with NaOH. Slices with a thickness of 200–250 μm were prepared as coronal sections on a vibratome. Slices were transferred to a holding chamber and kept submerged (at 30 °C for 30 min, thereafter at room temperature) in artificial cerebrospinal fluid (ACSF) containing (in mM): NaCl (125), KCl (2.5), NaH_2PO_4 (1.25), $NaHCO_3$ (24), $MgSO_4$ (2), $CaCl_2$ (2), dextrose (10), pH adjusted to 7.34 by bubbling with carbogen (95% O_2 and 5% CO_2 gas mixture).

The electrical properties of cortical pyramidal cells were determined in current clamp mode. The characteristics of the cell membrane were measured through glass microelectrodes pulled from borosilicate glass

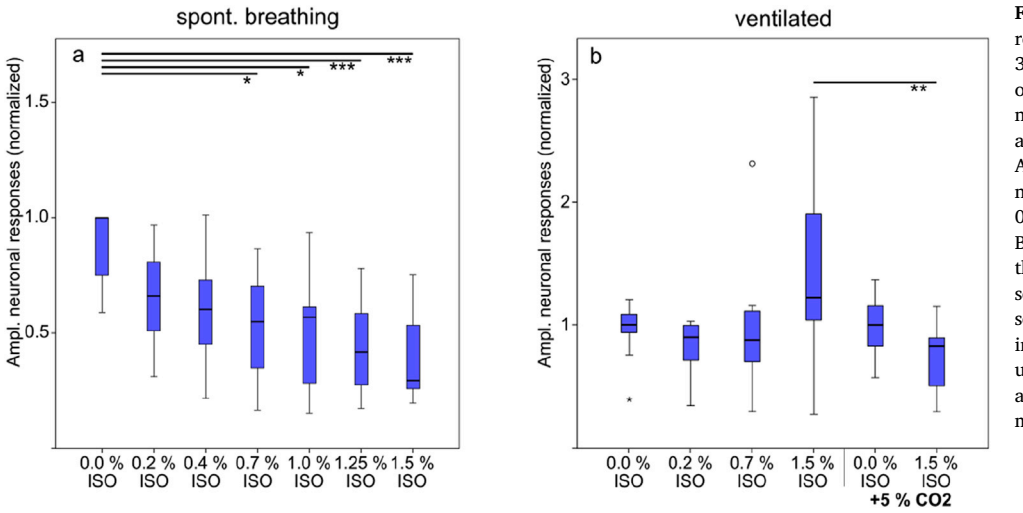

Fig. 4. Amplitudes of neural responses represented as boxplots (for stimulation with 3 Hz), normalized to the mean amplitudes occurring at pure MED sedation for spontaneously breathing animals (**a**) and ventilated animals (**b**).
Addition of CO_2 had no effect on this phenomenon ($p = 1.0$). * ≙ $p < 0.05$; ** ≙ $p < 0.01$; *** ≙ $p < 0.001$.
Boxplots represent data between first and third quartiles, the band in the box marks the second quartile (=median). Whiskers represent lowest and highest data within 1.5 interquartile ranges (IQR) of the lower and upper quartile. Outliers within 1.5 and 3 IQR are marked as dots, values outlying 3 IQR are marked stars.

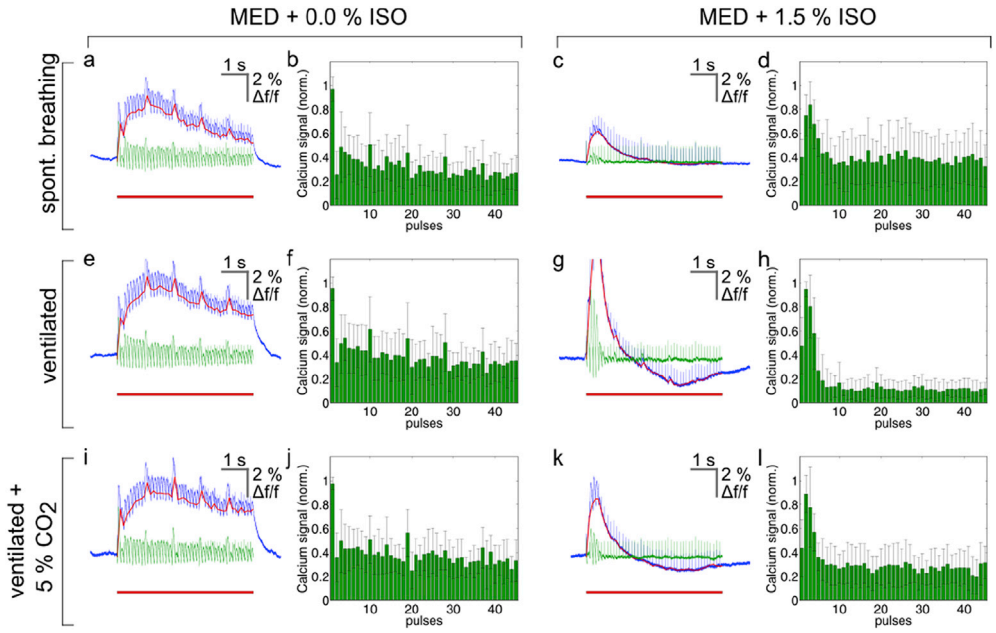

Fig. 5. Averaged calcium traces for stimulation with 9 Hz from spontaneously breathing animals under pure MED sedation (**a**) and with 1.5% ISO in addition (**c**), from ventilated animals without (**e**) and with 1.5% ISO (**g**) and from ventilated animals that obtained MED and additionally CO_2 in the inspiratory air (**i**), plus ISO (**k**). (**b,d,f,h,j** and **l**) are the corresponding amplitudes (normalized to the highest amplitude in the stimulation period).

capillaries (GC150T-10; Clark Electromedical Instruments, Pangbourne, UK) containing a chlorinated silver wire and filled with electrolyte solution (in mM): K-gluconate (95), K_3-citrate (20), NaCl (10), HEPES (10), $MgCl_2$ (1), $CaCl_2$ (0.5), BAPTA (3), Mg-ATP (3), Na_2-GTP (0.5). pH of 7.25 and an osmolality of 295 mOsm/kg. The patch electrode was connected to an EPC-10 amplifier (HEKA Elektronik, Lamprecht, Germany). Electrode resistances were in the range of 2.5–3.5 MΩ. Series resistance compensation of >30% was routinely applied. Experiments were controlled by the Pulse software (HEKA Elektronik).

For in vitro recordings, Dex-MED instead of MED was used. Dex-MED and MED have almost similar therapeutical effects (Ansah et al., 1998). Since potency and efficacy of Dex-MED is higher compared to MED, it is more efficient in slice recordings.

In a first step, we evaluated the effect of ISO and dexmedetomidine (Dex-MED; Dexomedetomidine hydrochloride, Sigma Aldrich, St. Louis, USA). To do so, we used a 1 Hz stimulation current clamp protocol. The protocol was composed of hyperpolarizing (−120 pA) and depolarizing (440 pA) current steps (1 s duration) with 40 pA increments. Recordings were done at 30–32 °C and perfusion rate of 2 ml/min in a solution containing (in mM): NaCl (125), KCl (2.5), NaH_2PO_4 (1.25), $NaHCO_3$ (24), $MgSO_4$ (2), $CaCl_2$ (2), dextrose (10). pH adjusted to 7.34 by bubbling with carbogen (5% CO_2 and 95% O_2). 10 μM Dex-MED and four concentrations of ISO were used for the measurements: 0.05%; 0.1%; 0.2% and 0.5 VOL%. ISO was dissolved in ACSF and mixed by ultrasonic baths sonicator (Bandelin SONOREX, RK255H, Germany). Recordings were performed from the resting membrane potential (RMP).

Matching in vivo concentrations for patch clamp experiments is not trivial. A detailed rationale for the concentrations chosen in this study is given in the supplementary material (Suppl. A).

Furthermore, according to the in vivo stimulation paradigm depolarizing current steps were applied at 3 Hz and 9 Hz (350 pA amplitude and 50 ms length) for 5 s duration and repeated for 10 times. In order to assess the effect of increased CO_2 concentrations, recordings were done in a solution containing (in mM): NaCl (120), KCl (2.5), NaH_2PO_4 (1.25),

HEPES (30), $MgSO_4$ (2), $CaCl_2$ (2), dextrose (10), pH = 7.34 adjusted with HCl, bubbled with 100% O_2 and subsequently carbogen (5% CO_2 and 95% O_2, pH = 6.8).

Data were analyzed offline using FitMaster (HEKA Elektronik) and Clampfit 10.7 (Axon Molecular Devices, Sunnyvale, California, USA) software and corrected for a liquid junction potential of 10 mV ($V_M = V_P$ – 10 mV; with V_M = membrane potential and V_P = pipette voltage). For a detailed overview of animals used for in vitro experiments see Suppl. Table 2.

2.5. Statistical analysis

Statistical analysis was conducted with SPSS (Version 24 [2016], IBM Corp., Armonk, NY, USA).

For in vivo experiments, data were checked for skewness with the Levene test. Analysis of homoscedasticity was performed with the Shapiro-Wilk test. Since normal distribution and homoscedasticity were not given for all subgroups, analysis of variance was performed with the Kruskal-Wallis test by ranks, followed by Dunn's post hoc test. Multiple comparison post-hoc correction was performed with Bonferroni correction. All significance levels denoted in this study are corrected for multiple comparisons. If different conditions were compared, relative values refer to the mean.

To test whether there were differences between SD and Fischer rats, pairwise comparisons for given conditions were conducted with Mann-Whitney-U-Test.

For in vitro experiments, analysis was performed with Repeated Measures ANOVA. Number of APs were used as dependent variable. Control, ISO, Dex-MED and CO_2 – as between subjects factor and current steps – within subject factor. Student's t-tests were used as post hoc tests, if necessary.

3. Results

3.1. BOLD fMRI

First, the impact of depth of anesthesia on the BOLD amplitude was investigated. In spontaneously breathing Fisher rats the highest BOLD amplitude occurred when animals were sedated with MED only (Fig. 2a, g and Suppl. Fig. 2a). If ISO was added, the amplitude diminished gradually with increasing ISO concentrations. For addition of 0.7% or higher concentrations of ISO the reduction of BOLD amplitude was significant ($p < 0.001$; compared to pure MED sedation). Results in SD rats were similar with no significant differences compared to Fisher rats (Suppl. Table 3).

In ventilated Fisher rats (Fig. 2c, d, h and Suppl. Fig. 2b), the observed decrease in BOLD amplitude upon addition of ISO (44% reduction for 1.5% ISO) was less pronounced than for spontaneously breathing animals. The decrease was not significant, which, however, may be due to larger confidence intervals as compared to the measurements in spontaneously breathing animals. Addition of 5% CO_2 in the breathing gas (Fig. 2e, f, h and Suppl. Fig. 2) resulted in a decrease of BOLD amplitude for both 0% and 1.5% ISO. While the reduction of 28% observed upon adding 5% CO_2 under 0% ISO was not significant ($p = 0.448$), the BOLD amplitude observed for 1.5% ISO and 5% CO_2 was significantly lower compared to all other conditions (Fig. 2f, h). All values are reported in Suppl. Table 4 and Suppl. Fig. 2.

Summarizing these results, we conclude that decrease of observed BOLD amplitude upon addition of ISO was only significant in spontaneously breathing animals but not in ventilated animals, under our experimental conditions. However, the combination of 1.5% ISO with 5% CO_2 (Fig. 2f, h) in ventilated animals reproduced the reduction of BOLD amplitude to a similar extent as administration of 1.5% ISO in spontaneously breathing animals. Standard deviation increased slightly in ventilated animals. Upon intubation we saw an increase in relative error (SD/mean) from 62% to 70%

3.2. Calcium recordings

Secondly, calcium responses in S1Fl to individual stimulation pulses were investigated. For stimulation with 3 Hz, the mean amplitude of individual calcium responses in spontaneously breathing animals declined when ISO was added. Amplitude reduction compared to pure MED sedation was significant for concentrations of 0.7% ISO ($p = 0.039$) and higher (1.5% ISO, 54% reduction, $p < 0.001$; Fig. 4a and Suppl. Fig. 3). For ventilated animals, addition of 1.5% ISO tended to increase the mean amplitude by 49% (n.s.), but no significant changes in amplitudes were observed for addition of ISO only, possibly due to larger confidence intervals (Suppl. Fig. 3). Addition of 5% CO_2 under 1.5% ISO, however, resulted in a significant effect. The amplitude declined by 49% compared to 1.5% ISO ($p = 0.004$; Fig. 4b, Suppl. Fig. 3). Relative error (SD/mean) in spontaneously breathing and ventilated animals were 35% and 38% in corresponding measurements.

This decrease in amplitude was not accompanied by changes in the peak shape of the responses. Full width at half maximum (FWHM) and onset, measured as time to half maximum did not change significantly for different inspiratory conditions neither in ventilated animals (FWHM: $p = 0.172$; onset: $p = 0.925$) nor in spontaneously breathing animals (FWHM: $p = 0.172$; onset: $p = 0.135$; data not shown).

For stimulation with 9 Hz, results were similar for spontaneously breathing animals with a significant reduction in amplitude compared to pure MED for 0.7% ISO and higher concentrations. In ventilated animals, no significant changes could be detected (data not shown). Next, alteration of neural responses during the 5 s duration of 9 Hz stimulation were studied. For pure MED sedation (Fig. 5b, f, j), the highest calcium responses appeared for the first stimulation pulse of each stimulation period. The more ISO was added, the more often the highest neural responses occurred later in one stimulation period (Fig. 5h). This shift of the highest peak due to administration of ISO was observed for both spontaneously breathing and ventilated animals, and was not affected by addition of CO_2 (Fig. 5d, l). For statistical analysis, we used the first five response peaks of each stimulation period. Apart from one single case, the highest amplitude appeared on the first pulse under pure MED sedation (mean = 1.20 ± 0.63; median = 1) in ventilated animals. With addition of 0.7% or 1.5% ISO, the highest amplitude rather occurred on the second (for 0.7%, $p = 0.012$ [compared to 0.0% ISO]) or third pulse (for 1.5%, $p = 0.004$ [compared to 0.0% ISO]).

The same trend was observed for spontaneously breathing rats. For pure MED sedation, the highest response peaks appeared following the first stimulus (mean = 1.17 ± 0.58; median = 1) and shifted when adding ISO. For addition of 1.5% ISO, the highest amplitude was observed following the third stimulus (mean = 3.0 ± 0.67; median = 3) – significantly later than under pure MED sedation ($p = 0.001$ [compared to 0.0% ISO]).

Besides peak amplitudes, different inspiratory conditions also had an impact on the observed baseline fluorescence (Fig. 5a and b, e, f, i, j; red line). To assess this effect, data were normalized for each animal and referenced to the amplitude of the baseline elevation which occurred for pure MED sedation at the end of each experiment. In spontaneously breathing animals, no relevant changes for different concentrations of ISO were observed (Fig. 6a). In ventilated animals, the induced baseline elevations became bigger with increasing ISO concentrations (Fig. 6b). For 1.5% ISO, they were on average about 4 times higher than under pure MED sedation (1.06 ± 0.74 for MED + 1.5% ISO vs. 4.02 ± 3.89 for MED sedation). Adding CO_2 on the other hand reduced the amplitude of the elevated baseline (MED + 1.5% ISO + 5% CO_2: 1.25 ± 1.11). Neither changes in spontaneously breathing nor in ventilated animals were statistically significant.

3.3. ASL

To separate the effects of both ISO and CO_2 on the vasculature from neural effects, perfusion was assessed by ASL measurements. In

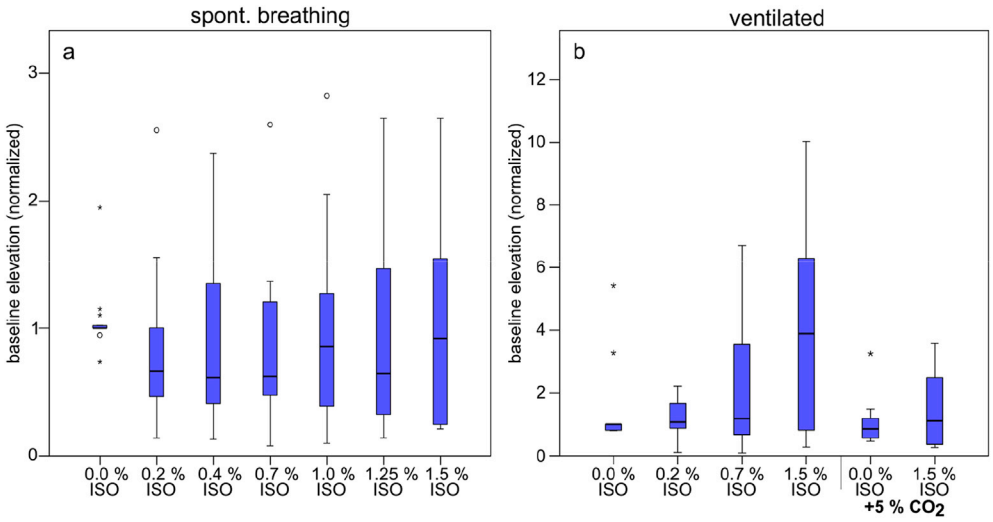

Fig. 6. Baseline elevation in calcium traces represented as boxplots. Baseline elevation during stimulation (with 9 Hz) in spontaneously breathing animals (**a**) and in ventilated animals (**b**). The increased range of results is a result of normalization to 0.0% ISO for each animal. Standard deviation of results does not increase in raw data.
Boxplots represent data between first and third quartiles, the band in the box marks the second quartile (=median). Whiskers represent lowest and highest data within 1.5 interquartile ranges (IQR) of the lower and upper quartile. Outliers within 1.5 and 3 IQR are marked as dots, values outlying 3 IQR are marked stars.

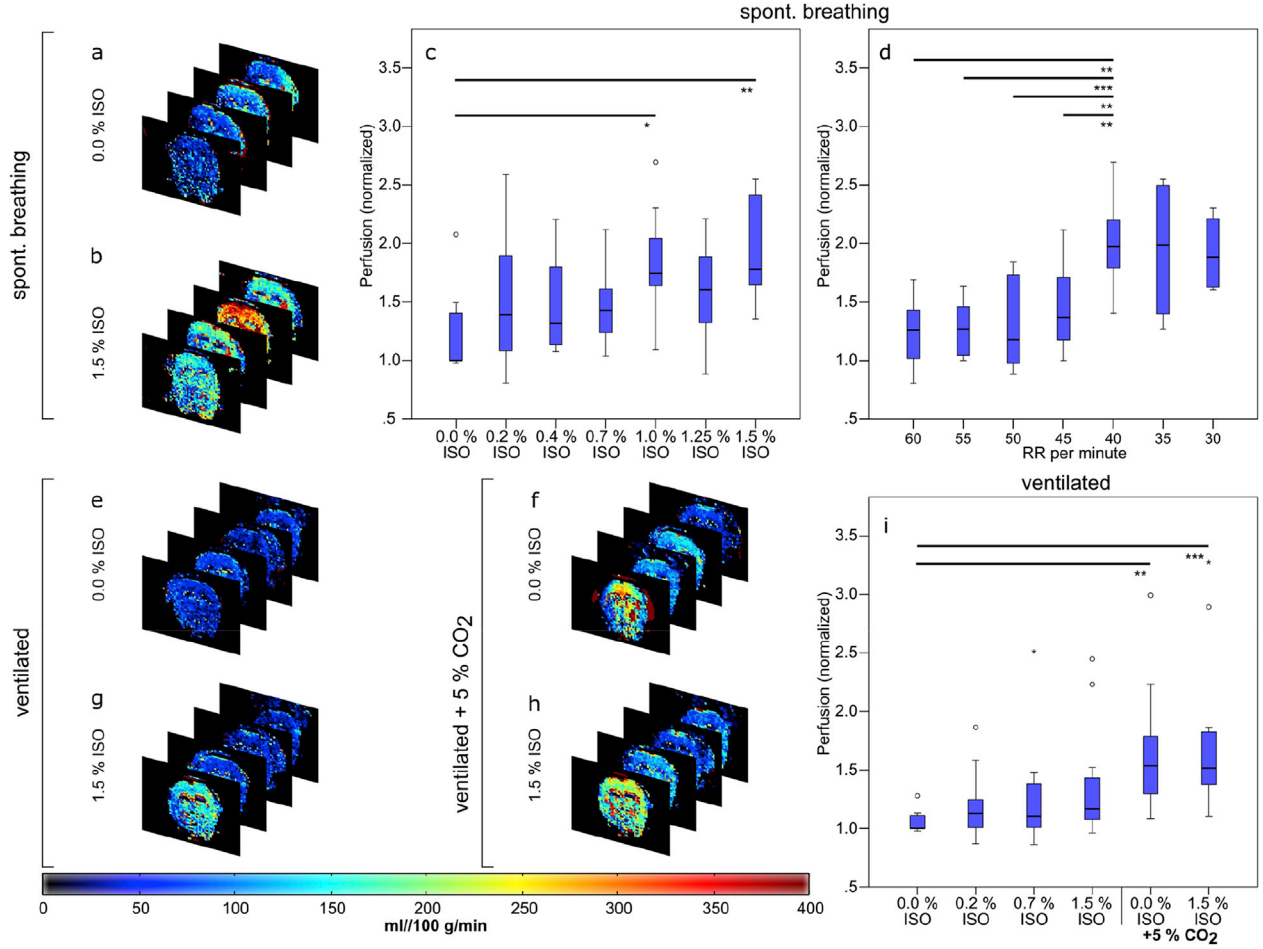

Fig. 7. Perfusion/ASL. Perfusion maps of spontaneously breathing animals without (**a**) and with (**b**) ISO. Boxplots of the normalized perfusion as a function of addition of ISO are given in (**c**), showing that ISO increased perfusion significantly as well as respiratory depression, that resulted from deeper anesthesia (**d**). Perfusion of ventilated animals (**e**) increased when ISO was added (**g**), but not significantly. If CO_2 was administered to the inspiratory air in ventilated animals (**f**) and if ISO and CO_2 were combined (**h**), perfusion increased significantly (**i**). The color bar indicates the level of perfusion.
Boxplots represent data between first and third quartiles, the band in the box stands for the second quartile (=median). Whiskers represent lowest and highest data within 1.5 interquartile ranges (IQR) of the lower and upper quartile. Outliers within 1.5 and 3 IQR are marked as dots, values outlying 3 IQR are marked stars.
* ≙ $p < 0.05$; ** ≙ $p < 0.01$; *** ≙ $p < 0.001$.

spontaneously breathing animals, we observed a concomitant increase in perfusion when ISO was added (Fig. 7a, b, c). However, this increase was only significant for relatively high doses of ISO (1.0% and 1.5%).

To avoid the influence of potentially anesthesia-dependent respiratory depression at higher ISO concentrations, we grouped the BOLD measurements according to the average respiratory rate (RR). The RR values at different ISO concentrations are reported in Suppl. Table 5. We assumed that RR is a surrogate marker for hypercapnia and thus correlated the grouped RR with perfusion (Fig. 7d). Even small reductions in RR (potentially due to deeper anesthesia) resulted in a significantly increased perfusion. In accordance with literature, we therefore made the assertion that hypoventilation and hypercapnia do have a significant influence on perfusion. This influence might be even bigger than direct effects of ISO.

Measurements in ventilated animals confirmed this assumption (Fig. 7e–i). Though addition of 1.5% ISO to MED sedation resulted in a perfusion increased by 30% on average, this increase was not significant ($p = 0.314$). Addition of 5% CO_2 to MED sedation however increased perfusion significantly by 57% ($p = 0.002$). Combining MED with 1.5% ISO and 5% CO_2 resulted in an increase of perfusion of 66% ($p < 0.001$).

3.4. Patch clamp recordings

Intrinsic membrane properties and electrical responses of cortical pyramidal cells were determined under current clamp recordings. Resting membrane potential (RMP) was measured about 5 min after establishing the whole cell configuration with zero current injection.

Although some nominal changes occurred in the RMP, no significant differences were found between control conditions and all ISO concentrations tested (Suppl. Table 6). 0.05% ISO did not change the RMP of the pyramidal cells (1 mV, $p = 0.83$; $n = 6$). While the RMP was slightly hyperpolarized by 0.1% (2 mV, $p = 0.23$; $n = 8$) and 0.2% ISO application (5 mV, $p = 0.388$; $n = 6$), higher concentrations of ISO (0.5%) depolarized the RMP of the pyramidal neurons (data not shown). Likewise, the R_{in} remained unchanged during all ISO concentrations used (0.05%: 71 MΩ, $p = 0.346$; $n = 6$; 0.1%: 3 MΩ, $p = 0.874$; $n = 8$; 0.2%: 48 MΩ, $p = 0.328$; $n = 6$).

Effects of ISO on intrinsic membrane excitability were investigated by 40–440 pA positive current injections. Dose-dependent suppression of action potentials (APs) firing was found for increasing concentrations of ISO. 0.05% ISO did not change the cell firing (Fig. 8a). 0.1% ISO caused moderate reduction in the number of APs (Figs. 8b) and 0.2% ISO resulted in complete suppression of firing in pyramidal neurons (Fig. 8c). In addition, a statistically different increase in the threshold of the first AP was found for 0.2% ISO (4.2 mV, $p = 0.037$; $n = 6$; Supp. Table 6).

Next, Dex-MED in a concentration of 10 μM was tested. While no significant effects were found for the RMP (1.3 mV hyperpoarization, $p = 0.65$; $n = 8$), R_{in} (15.5 MΩ decrease, $p = 0.477$; $n = 8$) and threshold of the first AP (2.5 mV increase, $p = 0.511$; $n = 8$; Suppl. Table 6), the number of APs was significantly decreased (Fig. 8d).

Subsequently, cortical slices were challenged with 10 μM Dex-MED in the presence of 0.1% ISO. As before, ISO slightly hyperpolarized the cell membrane (2 mV, $p = 0.6$; $n = 7$) and further hyperpolarization was found with Dex-MED application (3.5 mV, $p = 0.157$; $n = 7$). The number of APs was decreased by 0.1% ISO, too, and further suppressed by Dex-MED (Fig. 8e).

In order to study the effects of extracellular CO_2 concentrations on the firing of pyramidal cortical neurons, we used HEPES buffered ASCF bubbled with 100% oxygen (0% CO_2; pH = 7.34; $n = 10$). Switching 100% oxygen gas to a gas mixture of 5% CO_2 and 95% O_2 decreased pH of the same solution (pH = 6.8; $n = 10$).

Increased extracellular acidification (by addition of 5% CO_2) reduced the number of APs compared to control condition (100% O_2; Fig. 8f).

In accordance with the in vivo experiments, cortical pyramidal cells were challenged with depolarizing current pulses (length 50 ms) elicited at 3 or 9 Hz (pulse length 5 s; Fig. 9a and b).

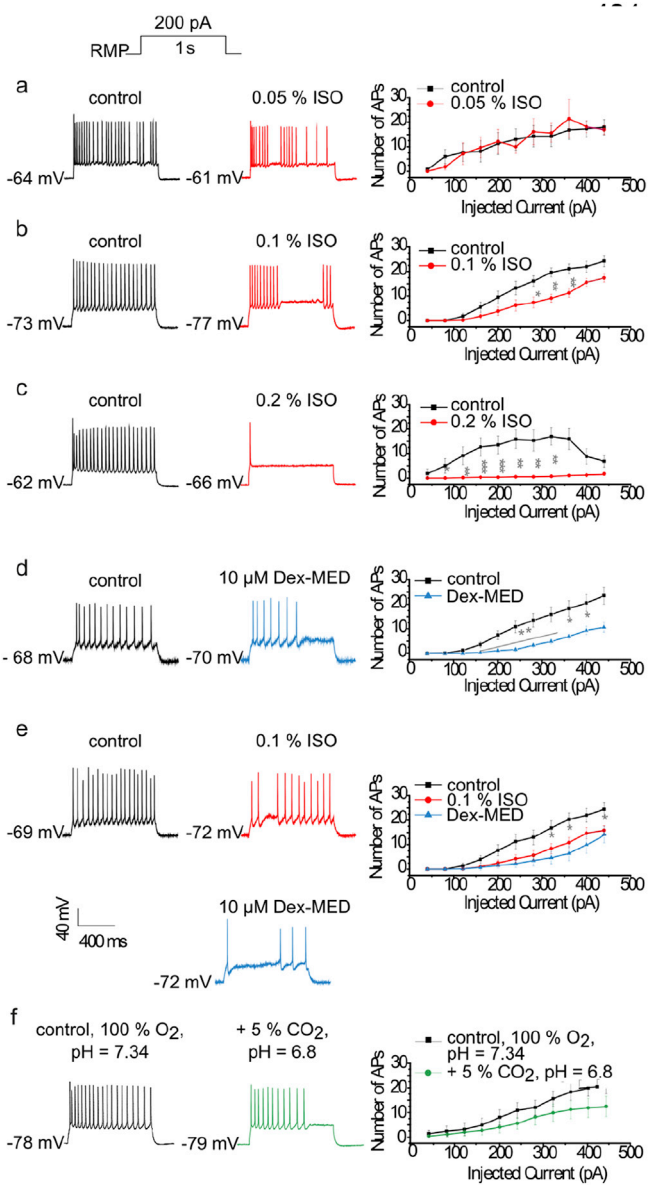

Fig. 8. Active membrane properties of the pyramidal cells under current clamp recordings. **(a)** Example traces of the pyramidal neurons injected with 200 pA depolarizing current during control (in black) and 0.05% ISO (in red) application (left panel). A series of depolarizing current injection induced almost the same numbers of AP in control (in black) and 0.05% ISO (in red) applied cells (right panel); **(b)** 0.1% ISO (in red) reduced the number of APs compared to control (in black) conditions; **(c)** The APs were suppressed by 0.2% ISO (in red), in comparison with control (in black); **(d)** 10 μM Dexomedetomine decreased the number of APs (in blue), compared to control (in black); **(e)** Washing the slices first with 0.1% ISO (in red) and then 10 μM Dexomedetomine (in blue) caused the reduction of the number of APs in comparison with control (in black) conditions: **(f)** Firing response of the cortex neurons to 5% CO_2. Extracellular acidification (in green) reduced the number of APs, compared to control alkalized (in black) condition.

Extracellular acidification resulted in decreased number of APs during both 3 and 9 Hz stimulations. To compare the results, the number of APs was calculated in percentage. The number of APs recorded under control conditions (100% O_2) was taken as 100% and the number of APs produced by 5% CO_2 application was calculated accordingly. 5% of CO_2 caused 10% reduction of APs during 3 Hz stimulation ($p = 0.259$; $n = 9$) and 20% reduction during 9 Hz stimulation ($p = 0.016$; $n = 6$).

Using the same stimulation paradigm, 0.1% ISO did not affect the

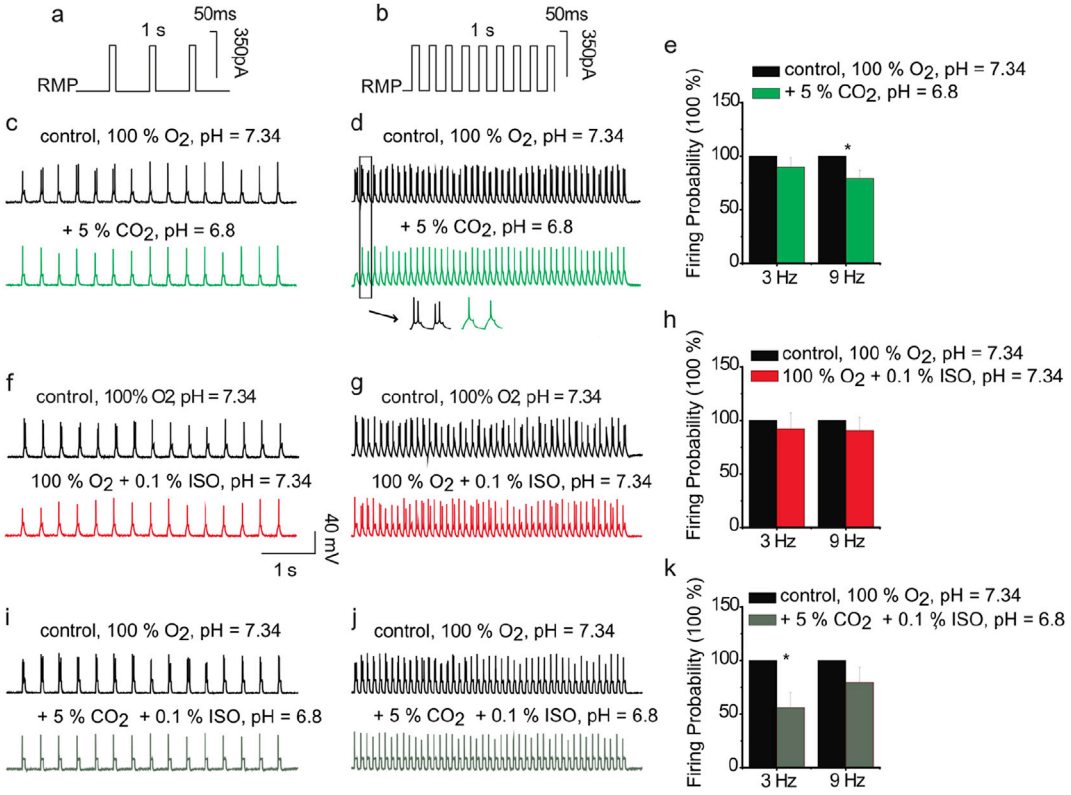

Fig. 9. Electrical responses of the pyramidal neurons under 3 and 9 Hz stimulation. 3 Hz **(a)** and 9 Hz (**b**) stimulation protocol contained 5 s of 50 ms 350 pA amplitude positive current injection; **(c–e)** The number of APs was decreased with low extracellular pH (pH = 6.8, in green), compared to mild alkalized (pH = 7.34, in black) condition; **(f–h)** 0.1% ISO (in red) decreased the cell excitability in comparison with control (in black); **(i–k)** In acidic extracellular solution (in gray) ISO significantly reduced the number of APs, compared to control (in black) solution.

number of APs significantly (Fig. 9f, g, h). The reduction in the number of APs was 8% ($p = 0.6$; $n = 7$) and 10% ($p = 0.478$; $n = 5$) during 3 Hz and 9 Hz stimulation, respectively. In the presence of 5% CO_2 the reduction of the number of spikes was stronger (3 Hz: 44%, $p = 0.013$; $n = 6$; 9 Hz: 21%, $p = 0.173$; $n = 7$; Fig. 9i, j, k).

4. Discussion

4.1. Basic pharmacological pathways

For interpretation of our results, it is necessary to consider the pharmacology of the agents used in this study. MED is an alpha-2-adrenoreceptor-agonist with sedative properties. Subtypes of alpha-2-receptors are known to regulate arousal and vigilance in the brainstem, and are further responsible for vasoconstrictive effects (Sinclair, 2003). Alpha-2-adrenoreceptor agonists hence have various effects such as bradycardia, analgesia and sedation (Scheinin et al., 1989). Compared to a previous study investigating functional connectivity (Grandjean et al., 2014), the dose of MED was considered to be rather low.

The pharmacology of volatile anesthetics, such as ISO, on the other hand, is poorly understood – despite its long use. Compared to MED, ISO is less selective, acting via different pharmacological pathways: a direct action on lipids as well as on defined proteins (Franks and Lieb, 1994) such as different ligand- and voltage-gated ion channels have been described (Daniels and Smith, 1993), as well as an activity-dependent depression of presynaptic voltage-gated sodium channels (Purtell et al., 2015). Furthermore, effects on various ligand-gated ion channels like $GABA_A$, 5-HT_3, NMDA, AMPA and nicotinic acetylcholine (ACh) receptors are discussed (Krasowski and Harrison, 1999).

ISO is also known to dilate cerebral vessels via ATP-sensitive K^+ channels (Iida et al., 1998) and to reduce cerebral vascular resistance (CVR) significantly (Leoni et al., 2011). Hypercapnia has a similar effect since it leads to increased CBF values (Jones et al., 2005; Leoni et al., 2011). In this study, we could detect both the effect of CO_2 and of ISO on vasculature, but only CO_2 triggered a statistically significant vasodilatation.

Increased neuronal activity enhances carbohydrate metabolism and decreases pH by producing lactic acid and CO_2 (Esquivel et al., 2010), but local endogenous hypercapnia following neural activity is not responsible for increased blood flow, as extracellular space is rather immediately alkalized through neuronal firing (Makani and Chesler, 2010). Exogenous CO_2 however does increase blood flow both in vivo (Jones et al., 2005; Leoni et al., 2011) and in vitro (Tian et al., 1995). The effects of pH changes on neuronal excitability are mediated by different voltage- and ligand-gated ion channels and gap junctions. Important players in cell excitability like inward rectifying potassium channels are inhibited by low extracellular pH values (Coulter et al., 1995). In addition to the family of acid-sensing ion channels (ASICs), a number of ion channels including voltage-activated K^+ channels, HCN channels, gap junction channels and Cl^- channels, alter their electrophysiological properties in response to pH changes. The voltage-gated Na^+ current amplitude is also decreased by low pH (Sun et al., 1997). In hippocampal pyramidal and in thalamic relay neurons, reduced extracellular pH decreases the peak of high and low voltage activated calcium current amplitude (Tombaugh and Somjen, 1996).

4.2. fMRI and ASL

Both calcium recordings and BOLD fMRI serve as a measure of neural activity. It was previously described that responses in electrophysiological measurements and BOLD are not necessarily coupled in a simple and linear manner in non-event related experiments (Schölvinck et al., 2010; Thompson et al., 2013) and event-related experiments (Franceschini et al., 2008). Schulz et al. (2012) on the other hand could predict BOLD

responses from simultaneously recorded calcium responses. Here, we showed that under certain anesthetic conditions, BOLD responses can be dissociated from neural activity present in calcium recordings.

In spontaneously breathing animals, even little addition of ISO was associated with a reduction of BOLD amplitude. High ISO concentrations (1.5%) fully suppressed the BOLD response. In ventilated animals, addition of ISO also resulted in a reduction of BOLD (not significant), but only the combination of ISO and CO_2 significantly suppressed the BOLD signal under our experimental conditions ($p < 0.001$, compared to 0% ISO and CO_2). This indicates that the reduction in BOLD amplitude in spontaneously breathing animals results from a combination of a direct effect of ISO and the impact of CO_2. When spontaneously breathing animals were anesthetized more deeply, respiratory depression caused accumulation of CO_2. Such suppression of BOLD could be reproduced by adding CO_2 to the inspiratory air in ventilated animals.

An important role of CO_2 for the BOLD signal was also corroborated by our measurements of perfusion. Addition of ISO increased perfusion in spontaneously breathing animals. However, the increase was significant only for high doses of ISO. The respiratory rate (as a surrogate marker for CO_2) was a better predictor for CBF than the dosage of ISO. There was no statistically significant effect of ISO on perfusion detectable in ventilated animals. Addition of CO_2, by contrast, resulted in a significant increase in CBF, irrespective of ISO concentration.

Potential bias due to time-dependent effects can largely be ruled out by the study design comprising two measurements per animal where possible, the first one early, the second one later in time. If data from earlier and later measurement were compared, a tendency towards higher BOLD responses in later measurements was observed. To detect systematic differences, we analyzed pairs of measurements at 0.0% ISO, 0.2% ISO and 0.7% ISO [data points separated by at least 1 h, available both in ventilated and spontaneously breathing animals and arranged symmetrically]. After correction for multiple comparisons problem, none of these differences was statistically significant [data not shown]. A detailed discussion of time-dependent effects of anesthesia is beyond the scope of this study and for example given by Magnuson et al. (2014).

4.3. Neural responses in calcium recordings and electrophysiology

In contrast to BOLD, calcium recordings can be considered as a more direct readout of neural activity in vivo. It is important to note that amplitudes of neural responses in calcium recordings cannot simply be compared between different experiments or animals, since the amplitude depends on different experimental conditions. Influencing factors comprise for example positioning of the fiber and level of expression of the calcium indicator itself. We therefore compared values which were normalized for each animal.

Although GCaMP6f is fast enough to resolve single neural responses at 9 Hz stimulation, it is not fast enough to reach a baseline fluorescence between two pulses since interpulse intervals of approximately 110 ms (= interpulse interval with 9 Hz stimulation) are too short (Chen et al., 2013). Since the interpulse intervals are longer for lower stimulation frequencies, superposition of calcium transients is weaker. We therefore primarily analyzed the mean amplitude to individual pulses at 3 Hz stimulation.

Looking at these amplitudes, the observed decrease in amplitude when ISO was added in spontaneously breathing animals, and when CO_2 was added in ventilated animals, was contrasted by a tendency to increasing the amplitude when 1.5% ISO was administered to ventilated animals. We conclude that the lower amplitude of pulse-evoked neural responses in spontaneously breathing animals was due to hypoventilation and thus due to an increased amount of CO_2, as in ventilated animals with administered CO_2 (Fig. 5). This reduction in amplitude in calcium recordings when CO_2 is added has an electrophysiological correlate, as the excitability is reduced. It is not clear, whether CO_2 itself or the acidification that it provokes is the main regressor. It was previously shown that pH impacts both transmitter release (presynaptically) and (postsynaptically) cell excitability (Sinning and Hübner, 2013).

We found that changes in extracellular pH (through administration of CO_2) affected the excitability of the pyramidal neurons and that extracellular acidification decreased the firing of the neurons. This "external" acidification has to be differentiated from the transient pH shift that happen during spontaneous neuronal activity and electrical stimulation in vitro (Chesler and Kaila, 1992). It has been found that in most brain regions (like the cortex) CO_2 decreases mean firing rate of neurons in vitro, although chemosensitive neurons from brain stem and hypothalamus are excited by CO_2 (Putnam et al., 2004; Williams et al., 2007). Our patch clamp experiments showed that the number of APs was decreased for administration of both CO_2 and ISO/Dex-MED if long lasting depolarizing current steps of 1 s duration were applied (Fig. 8). For pulsed stimulation (with 3 or 9 Hz, similar to our in vivo experiments) the number of APs per stimulation pulse was decreased by addition of CO_2, but not significantly for addition of ISO (Fig. 9). As fiber-based calcium recordings integrate signal of 20–100 neurons (Grienberger et al., 2012), a reduced number of APs, as observed by patch clamp recordings, is expected to result in a smaller amplitude of the in vivo calcium signal. However, no uniform trend for gradually increasing doses of ISO or adding CO_2 was observed in in vivo calcium recordings in ventilated animals, suggesting that a complex interplay of different factors impacts the detected signal. Volatile anesthetics like ISO, enflurane and halothane depress spontaneous action potential firing of neocortical neurons in a concentration-dependent manner (Kendig, 2002). Spontaneous single and multi-unit activity in cultured neocortical slices decrease the mean firing rates by enhancing $GABA_A$ receptor-function and decreasing glutamatergic synaptic transmission (Westphalen and Hemmings, 2003). We hypothesize that ISO leads to a generally lower excitability of the whole ensemble under observation, leading to less spontaneous background activity, while background activity is higher under MED. Evoked calcium responses, therefore, may result in higher amplitudes, since signal is always detected relative to the background signal of the ensemble.

van Hulzen and Coenen (1984) reported that the amplitude of Event Related Potentials in EEG is significantly higher in sleeping than in awake rats. Coenen (1995) interpreted that this was due to higher synchronicity. Grienberger et al. (2012) further observed that the amplitude of fast responses to sensory stimuli is smaller, if the level of fluorescence at stimulus onset is higher. Our data showed more spontaneous activity (Fig. 4a, e) when animals were only sedated (with MED), compared to anesthetized rats (with ISO; Fig. 4b, f). This observation is in line with the notion that more neurons are engaged in spontaneous activity, and consequently less neurons are available to fire synchronously in response to a stimulus. On the contrary, under ISO anesthesia the probability for neurons to be engaged in spontaneous activity is lower and thus more neurons may be available to fire synchronously. Sensory stimuli may thus evoke higher calcium responses. On a conceptual level, Northoff et al. (2010) already pointed out that the brain's intrinsic activity modulates stimulus-evoked activity.

Our observations are in accordance to burst suppression patterns in EEG-recordings evoked by ISO. Kroeger and Amzica (2007) stated that the burst suppression state provoked by deep anesthesia is a state of cortical hyperexcitability, This was most probably due to reduction of cortical inhibition (Ferron et al., 2009). During anesthesia, a corresponding increased tendency of thalamocortical neurons for burst firing and synchronous activity was observed (Budde et al., 2008). It is important to note that these findings were obtained by in vivo electrophysiological recordings. They likely describe the same phenomenon, but calcium and eletrophysiological patterns in vivo do not necessarily correlate in a simple way.

This notion is also corroborated by previous observations on the network level. Kalthoff et al. (2013) reported reliable networks in cortex and striatum under MED sedation which were drastically reduced under ISO anesthesia whereas Paasonen et al. (2017) reported good correlation values under ISO and under MED anesthesia. Peltier et al. (2005) observed reduced functional connectivity with deeper anesthesia in

humans. It was also described that specific sleep-like brain states that could be provoked by anesthesia come along with altered corticocortical and corticothalamic connectivity (Zhurakovskaya et al., 2016). These could be correlatives to our findings, that spontaneous activity is reduced with increasing doses of ISO.

4.4. Adaptation of neural responses, baseline elevation and decoupling

Over the 5 s period of stimulation, we observed a rapid adaptation of neural responses, especially for 9 Hz stimulation in the calcium recordings. Neural adaptation was previously described in electrophysiological measurements (Musall et al., 2014) and in optical calcium recordings (Schmid et al., 2016; Schulz et al., 2012) with an increasing adaptation index for higher stimulation frequencies. Patch clamp experiments also showed that the normalized response to a 9 Hz stimulation paradigm was lower than for 3 Hz stimulation. This suggests that there is indeed an electrophysiological correlate to smaller responses to 9 Hz stimulation in the calcium signal and that this is not an exclusive effect of limited temporal resolution of GCaMP6f in the first place (Fig. 6, Suppl. Fig. 4). We did not find a hemodynamic correlate to this altered neural adaptation. This could be due to the slow hemodynamic response. However, it does not necessarily mean that there is no altered adaptation in the BOLD signal since the temporal resolution of the BOLD signal in this study was 1 Hz (TR = 1s). O'Herron et al. (2016) found that vessels often responded robustly to stimuli while surrounding neural tissue did not. Aksenov et al. (2016) and Schmid et al. (2016) found that local neural and hemodynamic signals can be decoupled in terms of adaptation to the length of the stimulation and to higher stimulation frequencies. Indeed, the amplitude of neural responses in the calcium signal could not predict the BOLD amplitude or vice versa in our study.

Besides alterations of amplitudes and adaptation of neural responses, we analyzed the elevation of baseline fluorescence over the stimulation period of 5 s. Higher ISO elevated the baseline in ventilated, but not in spontaneously breathing animals, although with great variance and therefore not statistically significant, In ventilated animals, baseline elevation concomitantly increased with higher ISO concentrations, while CO_2 abolished this effect. Spontaneously breathing animals had a lower respiration rate at high concentrations of anesthetics. Consequently, we assume that both an increased amount of ISO and of CO_2 affecting the brain and mutually counteracting each other, an effect possibly based on the differential effect repertoire of both compounds. Indeed TASK channels (which are strongly expressed in thalamic and neocortical neurons) are activated by ISO and inhibited by extracellular acidification (Budde et al., 2008; Duprat et al., 1997; Rajan et al., 2000; Talley et al., 2001). In thalamocortical neurons, extracellular acidification leads to simultaneous inhibition of currents through TASK and HCN channels thereby limiting changes in membrane potential and neuronal excitability (Meuth et al., 2003, 2006).

As pointed out by Grienberger and Konnerth (2012), calcium indicators measure alterations of the calcium concentration in the cytosol, as a product of calcium efflux and influx. Grienberger et al. (2012) reported a fast response to a sensory stimulus and following the fast response a second, slow component, which was closely linked to slow membrane potential oscillations from a 'hyperpolarized down state' to the 'depolarized up state'. In patch clamp experiments, the normalized response to 9 Hz stimulation was significantly lower than to 3 Hz stimulation (Suppl. Fig. 4), indicating that the time between two pulses at 9 Hz is indeed not sufficient for the neuron to regain a full state of rest and full excitability, defining the slow component of the calcium signal. This may also explain the different responses observed for continuous application of current for 1 s (Fig. 8) and pulsed application of electrical current (Fig. 9). We assume that different anesthetics have different impacts on the slow component. The "undershoot", a decreased level of baseline fluorescence (Fig. 5g, k) compared to the baseline without stimulation may be an indication that ISO affects subcellular structures to different extent, which might be for example a reduced effectivity of calcium efflux pumps.

4.5. Neurovascular coupling and synopsis

Our data show in accordance with literature that anesthesia has distinct effects on both neural signal and on vasculature. It was long thought that increase of neural activity simply triggers a metabolic response that provokes a blood flow increase (Attwell et al., 2010). The majority of cortical energy production supports glutamatergic neuronal signalling (Sibson et al., 1998). A release of glutamate interacts with neuronal NMDA receptors and leads to production of nitric oxide, known for dilating cerebral vessels (Busija et al., 2007). There is also evidence that other neurotransmitters and corresponding receptors may be involved in neurovascular coupling, comprising $GABA_A$ (Kocharyan et al., 2008; Vaucher et al., 2000), lactate (Gordon et al., 2008; Lauritzen et al., 2014), noradrenaline (Bekar et al., 2012) and others.

Since volatile anesthetics affect ligand-gated ion channels (Krasowski and Harrison, 1999), lactate signalling (Horn and Klein, 2010) as well as noradrenergic projections (Vazey and Aston-Jones, 2014) and various other pathways, altered neurovascular coupling is highly likely. Interpreting results of different modalities as a whole is difficult, especially a direct comparison between fMRI read out and cell firing features. While fMRI provides an indirect readout of the activity of neuronal populations, whole cell current clamp recordings give information about the single cell activity. This does not necessarily mean that deeper anesthesia triggers decoupling. A previous study reported a tight EEG-CBF correlation in a deeply anesthetized brain (Liu et al., 2011) investigating spontaneous EEG and CBF changes. Nevertheless, when experimental parameters affect BOLD signal as well as intracellular Ca^{2+} dynamics and AP generation in the same direction, an inference to the main source of interest, the neuronal activity seems to be likely.

BOLD fMRI and optical calcium recordings are invaluable tools for measuring neural activity in vivo. But care must be taken for design of such studies since anesthesia can have opposing effects on calcium recordings and BOLD signal. It can result in decreasing BOLD when the calcium signal is increased and vice versa. Calcium recordings must not be seen as a summation of activity of equally behaving neurons, but of neurons that are part of a network with its own characteristics, including spontaneous activity. Behaviour of individual patch-clamped neurons in vitro can thus not predict the behaviour of neural populations in vivo.

5. Conclusion

The most important result of the present study is that anesthesia is eligible to cause dissociation between hemodynamic BOLD response and neural activity in the calcium signal. The BOLD response cannot generally predict neural responses in the calcium signal and vice versa. Calcium recordings in vivo and patch clamp experiments in vitro are also affected differently, because spontaneous, non-event-related activity impacts event-related responses.

Already low doses of anesthesia affect each physiological component underlying the BOLD signal to various extents. Consequently, animals should be anesthetized as slightly as possible. Care must be taken to ensure physiological conditions. Animals react in different ways to the application of anesthetics and they react individually, e.g. with great deviations concerning the drop in respiration rate. If the study design comprises spontaneously breathing animals, one must consider both the effect of anesthetics and CO_2 due to respiratory depression. Uncontrolled levels of CO_2 may be avoided if ventilated animals are used. Simultaneously, the expiratory CO_2 should be controlled narrowly. With BOLD fMRI alone, it is not possible to estimate the effects of the anesthesia applied. The combination of BOLD fMRI and calcium recordings in vivo is an excellent tool for mapping and analyzing neural activity. It does not only combine the inherent advantages of both techniques, but the combination is also giving additional information about the characteristics of brain networks under tightly defined experimental conditions.

Acknowledgement

We thank the medical faculty of the University of Münster for financial support. This work was funded in part by the Interdisciplinary Center for Clinical Research Münster (Fa3/016/13 and Bud3/001/16) and the German Research Foundation (Fa474/5 and BU1019/15-1). None of the funding sources was involved in study design, collection, analysis and interpretation of data. We thank Annika Lüttjohann and Henriette Lambers for valuable comments and Florian Schmid for his work on the establishment of parallel acquisition of BOLD and calcium recordings in our lab.

Appendix A. Supplementary data

Supplementary data to this article can be found online at https://doi.org/10.1016/j.neuroimage.2019.03.057.

Author contributions

T.v.A. and C.F. designed the study. T.v.A., L.W. and F.A. conducted ASL, fMRI and Ca^{2+} experiments. M.D. and T.B. conducted patch clamping experiments. N.J. established the FAIR-RARE procedures. T.v.A. analyzed the data. T.v.A, T.B., M.D. and C.F. wrote the manuscript. All authors edited the manuscript.

Conflicts of interest

None.

Ethics statement

All experiments were performed according to the German Tierschutzgesetz and were approved by local authorities (Landesamt für Natur, Umwelt und Verbraucherschutz Nordrhein-Westfalen, Germany [approval ID 84–02.04.2015.A427 and 84–02.04.2014.A347 for in vivo experiments; 84–02.05.50.15.026 for in vitro/patch clamp experiments]).

References

Akerboom, J., Chen, T.-W., Wardill, T.J., Tian, L., Marvin, J.S., Mutlu, S., Calderón, N.C., Esposti, F., Borghuis, B.G., Sun, X.R., Gordus, A., Orger, M.B., Portugues, R., Engert, F., Macklin, J.J., Filosa, A., Aggarwal, A., Kerr, R.A., Takagi, R., Kracun, S., Shigetomi, E., Khakh, B.S., Baier, H., Lagnado, L., Wang, S.S.-H., Bargmann, C.I., Kimmel, B.E., Jayaraman, V., Svoboda, K., Kim, D.S., Schreiter, E.R., Looger, L.L., 2012. Optimization of a GCaMP calcium indicator for neural activity imaging. J. Neurosci.: Offic. J. Soc. Neurosci 32, 13819–13840. https://doi.org/10.1523/JNEUROSCI.2601-12.2012.

Aksenov, D.P., Li, L., Miller, M.J., Iordanescu, G., Wyrwicz, A.M., 2015. Effects of anesthesia on BOLD signal and neuronal activity in the somatosensory cortex. J. Cereb. Blood Flow Metab.: Offc. J. Int. Soc. Cereb. Flow. Metabol. 35, 1819–1826. https://doi.org/10.1038/jcbfm.2015.130.

Aksenov, D.P., Li, L., Miller, M.J., Wyrwicz, A.M., 2016. Blood oxygenation level dependent signal and neuronal adaptation to optogenetic and sensory stimulation in somatosensory cortex in awake animals. Eur. J. Neurosci. 44, 2722–2729. https://doi.org/10.1111/ejn.13384.

Albers, F., Wachsmuth, L., van Alst, T.M., Faber, C., 2018. Multimodal functional neuroimaging by simultaneous BOLD fMRI and fiber-optic calcium recordings and optogenetic control. Mol. Imag. Biol.: MIB:Offc. Pub. Acad. Molecul. Imag. 20, 171–182. https://doi.org/10.1007/s11307-017-1130-6.

Ansah, O.B., Raekallio, M., Vainio, O., 1998. Comparison of three doses of dexmedetomidine with medetomidine in cats following intramuscular administration. J. Vet. Pharmacol. Ther. 21, 380–387. https://doi.org/10.1046/j.1365-2885.1998.00155.x.

Attwell, D., Buchan, A.M., Charpak, S., Lauritzen, M., Macvicar, B.A., Newman, E.A., 2010. Glial and neuronal control of brain blood flow. Nature 468, 232–243. https://doi.org/10.1038/nature09613.

Bekar, L.K., Wei, H.S., Nedergaard, M., 2012. The locus coeruleus-norepinephrine network optimizes coupling of cerebral blood volume with oxygen demand. J. Cereb. Blood Flow Metab.: Offc. J. Int. Soc. Cereb. Flow. Metabol. 32, 2135–2145. https://doi.org/10.1038/jcbfm.2012.115.

Berwick, J., Martin, C., Martindale, J., Jones, M., Johnston, D., Zheng, Y., Redgrave, P., Mayhew, J., 2002. Hemodynamic response in the unanesthetized rat: intrinsic optical imaging and spectroscopy of the barrel cortex. J. Cereb. Blood Flow Metab.: Offc. J. Int. Soc. Cereb. Flow. Metabol. 22, 670–679. https://doi.org/10.1097/00004647-200206000-00005.

Brynildsen, J.K., Hsu, L.-M., Ross, T.J., Stein, E.A., Yang, Y., Lu, H., 2017. Physiological characterization of a robust survival rodent fMRI method. Magnet. Reson. Imag. 35, 54–60. https://doi.org/10.1016/j.mri.2016.08.010.

Budde, T., Coulon, P., Pawlowski, M., Meuth, P., Kanyshkova, T., Japes, A., Meuth, S.G., Pape, H.-C., 2008. Reciprocal modulation of I (h) and I (TASK) in thalamocortical relay neurons by halothane. Pflueg. Arch. Eur. J. Physiol. 456, 1061–1073. https://doi.org/10.1007/s00424-008-0482-9.

Busija, D.W., Bari, F., Domoki, F., Louis, T., 2007. Mechanisms involved in the cerebrovascular dilator effects of N-methyl-d-aspartate in cerebral cortex. Brain Res. Rev. 56, 89–100. https://doi.org/10.1016/j.brainresrev.2007.05.011.

Chen, T.-W., Wardill, T.J., Sun, Y., Pulver, S.R., Renninger, S.L., Baohan, A., Schreiter, E.R., Kerr, R.A., Orger, M.B., Jayaraman, V., Looger, L.L., Svoboda, K., Kim, D.S., 2013. Ultrasensitive fluorescent proteins for imaging neuronal activity. Nature 499, 295–300. https://doi.org/10.1038/nature12354.

Chesler, M., Kaila, K., 1992. Modulation of pH by neuronal activity. Trends Neurosci. 15, 396–402. https://doi.org/10.1016/0166-2236(92)90191-A.

Coenen, A.M., 1995. Neuronal activities underlying the electroencephalogram and evoked potentials of sleeping and waking: implications for information processing. Neurosci. Biobehav. Rev. 19, 447–463. https://doi.org/10.1016/0149-7634(95)00010-C.

Coulter, K.L., Périer, F., Radeke, C.M., Vandenberg, C.A., 1995. Identification and molecular localization of a pH-sensing domain for the inward rectifier potassium channel HIR. Neuron 15, 1157–1168. https://doi.org/10.1016/0896-6273(95)90103-5.

Daniels, S., Smith, E.B., 1993. Effects of general anaesthetics on ligand-gated ion channels. Br. J. Anaesth. 71, 59–64.

Driencourt, L., Romero, C.J., Lepore, M., Eggenschwiler, F., Reynaud, O., Just, N., 2017. T1 mapping of the mouse brain following fractionated manganese administration using MP2RAGE. Brain Struct. Funct. 222, 201–214. https://doi.org/10.1007/s00429-016-1211-3.

Duprat, F., Lesage, F., Fink, M., Reyes, R., Heurteaux, C., Lazdunski, M., 1997. TASK, a human background K+ channel to sense external pH variations near physiological pH. EMBO J. 16, 5464–5471. https://doi.org/10.1093/emboj/16.17.5464.

Ekstrom, A., 2010. How and when the fMRI BOLD signal relates to underlying neural activity: the danger in dissociation. Brain Res. Rev. 62, 233–244. https://doi.org/10.1016/j.brainresrev.2009.12.004.

Esquivel, G., Schruers, K.R., Maddock, R.J., Colasanti, A., Griez, E.J., 2010. Acids in the brain: a factor in panic? J. Psychopharmacol. 24, 639–647. https://doi.org/10.1177/0269881109104847.

Ferron, J.-F., Kroeger, D., Chever, O., Amzica, F., 2009. Cortical inhibition during burst suppression induced with isoflurane anesthesia. J. Neurosci.: Offic. J. Soc. Neurosci 29, 9850–9860. https://doi.org/10.1523/JNEUROSCI.5176-08.2009.

Franceschini, M.A., Nissilä, I., Wu, W., Diamond, S.G., Bonmassar, G., Boas, D.A., 2008. Coupling between somatosensory evoked potentials and hemodynamic response in the rat. Neuroimage 41, 189–203. https://doi.org/10.1016/j.neuroimage.2008.02.061.

Franks, N.P., Lieb, W.R., 1994. Molecular and cellular mechanisms of general anaesthesia. Nature 367, 607–614. https://doi.org/10.1038/367607a0.

Fukuda, M., Vazquez, A.L., Zong, X., Kim, S.-G., 2013. Effects of the α_2-adrenergic receptor agonist dexmedetomidine on neural, vascular and BOLD fMRI responses in the somatosensory cortex. Eur. J. Neurosci. 37, 80–95. https://doi.org/10.1111/ejn.12024.

Gao, Y.-R., Ma, Y., Zhang, Q., Winder, A.T., Liang, Z., Antinori, L., Drew, P.J., Zhang, N., 2017. Time to wake up: studying neurovascular coupling and brain-wide circuit function in the un-anesthetized animal. Neuroimage 153, 382–398. https://doi.org/10.1016/j.neuroimage.2016.11.069.

Gordon, G.R.J., Choi, H.B., Rungta, R.L., Ellis-Davies, G.C.R., Macvicar, B.A., 2008. Brain metabolism dictates the polarity of astrocyte control over arterioles. Nature 456, 745–749. https://doi.org/10.1038/nature07525.

Grandjean, J., Schroeter, A., Batata, I., Rudin, M., 2014. Optimization of anesthesia protocol for resting-state fMRI in mice based on differential effects of anesthetics on functional connectivity patterns. Neuroimage 102 (2), 838–847. https://doi.org/10.1016/j.neuroimage.2014.08.043.

Grienberger, C., Adelsberger, H., Stroh, A., Milos, R.-I., Garaschuk, O., Schierloh, A., Nelken, I., Konnerth, A., 2012. Sound-evoked network calcium transients in mouse auditory cortex in vivo. J. Physiol 590, 899–918. https://doi.org/10.1113/jphysiol.2011.222513.

Grienberger, C., Konnerth, A., 2012. Imaging calcium in neurons. Neuron 73, 862–885. https://doi.org/10.1016/j.neuron.2012.02.011.

Heeger, D.J., Ress, D., 2002. What does fMRI tell us about neuronal activity? Nat. Rev. Neurosci. 3, 142–151. https://doi.org/10.1038/nrn730.

Hillman, E.M.C., 2014. Coupling mechanism and significance of the BOLD signal: a status report. Annu. Rev. Neurosci. 37, 161–181. https://doi.org/10.1146/annurev-neuro-071013-014111.

Horn, T., Klein, J., 2010. Lactate levels in the brain are elevated upon exposure to volatile anesthetics: a microdialysis study. Neurochem. Int. 57, 940–947. https://doi.org/10.1016/j.neuint.2010.09.014.

Iida, H., Ohata, H., Iida, M., Watanabe, Y., Dohi, S., 1998. Isoflurane and sevoflurane induce vasodilation of cerebral vessels via ATP-sensitive K+ channel activation. Anesthesiology 89, 954–960.

Jones, M., Berwick, J., Hewson-Stoate, N., Gias, C., Mayhew, J., 2005. The effect of hypercapnia on the neural and hemodynamic responses to somatosensory stimulation. Neuroimage 27, 609–623. https://doi.org/10.1016/j.neuroimage.2005.04.036.

Kalthoff, D., Po, C., Wiedermann, D., Hoehn, M., 2013. Reliability and spatial specificity of rat brain sensorimotor functional connectivity networks are superior under sedation compared with general anesthesia. NMR Biomed. 26, 638–650. https://doi.org/10.1002/nbm.2908.

Kendig, J.J., 2002. In vitro networks: subcortical mechanisms of anaesthetic action. Br. J. Anaesth. 89, 91–101. https://doi.org/10.1093/bja/aef158.

Kocharyan, A., Fernandes, P., Tong, X.-K., Vaucher, E., Hamel, E., 2008. Specific subtypes of cortical GABA interneurons contribute to the neurovascular coupling response to basal forebrain stimulation. J. Cereb. Blood Flow Metab.: Offc. J. Int. Soc. Cereb. Flow. Metabol. 28, 221–231. https://doi.org/10.1038/sj.jcbfm.9600558.

Krasowski, M.D., Harrison, N.L., 1999. General anaesthetic actions on ligand-gated ion channels. Cell. Mol. Life Sci.: CM 55, 1278–1303. https://doi.org/10.1007/s000180050371.

Kroeger, D., Amzica, F., 2007. Hypersensitivity of the anesthesia-induced comatose brain. J. Neurosci.: Offic. J. Soc. Neurosci 27, 10597–10607. https://doi.org/10.1523/JNEUROSCI.3440-07.2007.

Lauritzen, K.H., Morland, C., Puchades, M., Holm-Hansen, S., Hagelin, E.M., Lauritzen, F., Attramadal, H., Storm-Mathisen, J., Gjedde, A., Bergersen, L.H., 2014. Lactate Receptor Sites Link Neurotransmission, Neurovascular Coupling, and Brain Energy Metabolism, vol. 24. Cerebral cortex, New York, N.Y., pp. 2784–2795. https://doi.org/10.1093/cercor/bht136, 1991.

Leoni, R.F., Paiva, F.F., Henning, E.C., Nascimento, G.C., Tannús, A., Araujo, D.B. de, Silva, A.C., 2011. Magnetic resonance imaging quantification of regional cerebral blood flow and cerebrovascular reactivity to carbon dioxide in normotensive and hypertensive rats. Neuroimage 58, 75–81. https://doi.org/10.1016/j.neuroimage.2011.06.030.

Liang, Z., Ma, Y., Watson, G.D.R., Zhang, N., 2017. Simultaneous GCaMP6-based fiber photometry and fMRI in rats. J. Neurosci. Methods 289, 31–38. https://doi.org/10.1016/j.jneumeth.2017.07.002.

Liu, X., Zhu, X.-H., Zhang, Y., Chen, W., 2011. Neural Origin of Spontaneous Hemodynamic Fluctuations in Rats under Burst-Suppression Anesthesia Condition, vol. 21. Cerebral cortex, New York, N.Y., pp. 374–384. https://doi.org/10.1093/cercor/bhq105, 1991.

Logothetis, N.K., 2008. What we can do and what we cannot do with fMRI. Nature 453, 869–878. https://doi.org/10.1038/nature06976.

Logothetis, N.K., Pauls, J., Augath, M., Trinath, T., Oeltermann, A., 2001. Neurophysiological investigation of the basis of the fMRI signal. Nature 412, 150–157. https://doi.org/10.1038/35084005.

Low, L.A., Bauer, L.C., Pitcher, M.H., Bushnell, M.C., 2016. Restraint training for awake functional brain scanning of rodents can cause long-lasting changes in pain and stress responses. Pain 157, 1761–1772. https://doi.org/10.1097/j.pain.0000000000000579.

Magnuson, M.E., Thompson, G.J., Pan, W.J., Keilholz, S.D., 2014. Time-dependent effects of isoflurane and dexmedetomidine on functional connectivity, spectral characteristics, and spatial distribution of spontaneous BOLD fluctuations. NMR Biomed. 27, 291–303. https://doi.org/10.1002/nbm.3062.

Makani, S., Chesler, M., 2010. Rapid rise of extracellular pH evoked by neural activity is generated by the plasma membrane calcium ATPase. J. Neurophysiol. 103, 667–676. https://doi.org/10.1152/jn.00948.2009.

Martin, C., Martindale, J., Berwick, J., Mayhew, J., 2006. Investigating neural-hemodynamic coupling and the hemodynamic response function in the awake rat. Neuroimage 32, 33–48. https://doi.org/10.1016/j.neuroimage.2006.02.021.

Masamoto, K., Kanno, I., 2012. Anesthesia and the quantitative evaluation of neurovascular coupling. J. Cereb. Blood Flow Metab.: Offc. J. Int. Soc. Cereb. Flow. Metabol. 32, 1233–1247. https://doi.org/10.1038/jcbfm.2012.50.

Meuth, S.G., Budde, T., Kanyshkova, T., Broicher, T., Munsch, T., Pape, H.-C., 2003. Contribution of TWIK-related acid-sensitive K+ channel 1 (TASK1) and TASK3 channels to the control of activity modes in thalamocortical neurons. J. Neurosci. : Offic. J. Soc. Neurosci 23, 6460–6469.

Meuth, S.G., Kanyshkova, T., Meuth, P., Landgraf, P., Munsch, T., Ludwig, A., Hofmann, F., Pape, H.-C., Budde, T., 2006. Membrane resting potential of thalamocortical relay neurons is shaped by the interaction among TASK3 and HCN2 channels. J. Neurophysiol. 96, 1517–1529. https://doi.org/10.1152/jn.01212.2005.

Musall, S., Behrens, W. von der, Mayrhofer, J.M., Weber, B., Helmchen, F., Haiss, F., 2014. Tactile frequency discrimination is enhanced by circumventing neocortical adaptation. Nat. Neurosci. 17, 1567–1573. https://doi.org/10.1038/nn.3821.

Nasrallah, F.A., Lee, E.L.Q., Chuang, K.-H., 2012. Optimization of flow-sensitive alternating inversion recovery (FAIR) for perfusion functional MRI of rodent brain. NMR Biomed. 25, 1209–1216. https://doi.org/10.1002/nbm.2790.

Northoff, G., Duncan, N.W., Hayes, D.J., 2010. The brain and its resting state activity–experimental and methodological implications. Prog. Neurobiol. 92, 593–600. https://doi.org/10.1016/j.pneurobio.2010.09.002.

O'Herron, P., Chhatbar, P.Y., Levy, M., Shen, Z., Schramm, A.E., Lu, Z., Kara, P., 2016. Neural correlates of single-vessel haemodynamic responses in vivo. Nature 534, 378–382. https://doi.org/10.1038/nature17965.

Paasonen, J., Salo, R.A., Huttunen, J.K., Gröhn, O., 2017. Resting-state functional MRI as a tool for evaluating brain hemodynamic responsiveness to external stimuli in rats. Magn. Reson. Med. 78, 1136–1146. https://doi.org/10.1002/mrm.26496.

Pawela, C.P., Biswal, B.B., Hudetz, A.G., Schulte, M.L., Li, R., Jones, S.R., Cho, Y.R., Matloub, H.S., Hyde, J.S., 2009. A protocol for use of medetomidine anesthesia in rats for extended studies using task-induced BOLD contrast and resting-state functional connectivity. Neuroimage 46, 1137–1147. https://doi.org/10.1016/j.neuroimage.2009.03.004.

Paxinos, G.T., Watson, C., 1997. The Rat Brain in Stereotaxic Coordinates: Hard, Cover Edition third ed. Acad. Press, San Diego, p. 78.

Peltier, S.J., Kerssens, C., Hamann, S.B., Sebel, P.S., Byas-Smith, M., Hu, X., 2005. Functional connectivity changes with concentration of sevoflurane anesthesia. Neuroreport 16, 285–288. https://doi.org/10.1097/00001756-200502280-00017.

Purtell, K., Gingrich, K.J., Ouyang, W., Herold, K.F., Hemmings, H.C., 2015. Activity-dependent depression of neuronal sodium channels by the general anaesthetic isoflurane. Br. J. Anaesth. 115, 112–121. https://doi.org/10.1093/bja/aev203.

Putnam, R.W., Filosa, J.A., Ritucci, N.A., 2004. Cellular mechanisms involved in CO(2) and acid signaling in chemosensitive neurons. Am. J. Physiol. Cell Physiol. 287, C1493–C1526. https://doi.org/10.1152/ajpcell.00282.2004.

Rajan, S., Wischmeyer, E., Xin Liu, G., Preisig-Müller, R., Daut, J., Karschin, A., Derst, C., 2000. TASK-3, a novel tandem pore domain acid-sensitive K+ channel. An extracellular histiding as pH sensor. J. Biol. Chem. 275, 16650–16657. https://doi.org/10.1074/jbc.M000030200.

Scheinin, H., Virtanen, R., MacDonald, E., Lammintausta, R., Scheinin, M., 1989. Medetomidine–a novel alpha 2-adrenoceptor agonist: a review of its pharmacodynamic effects. Prog. neuro-psychopharmacol. biol. psychiatr. 13, 635–651.

Schlegel, F., Sych, Y., Schroeter, A., Stobart, J., Weber, B., Helmchen, F., Rudin, M., 2018. Fiber-optic implant for simultaneous fluorescence-based calcium recordings and BOLD fMRI in mice. Nat. Protoc. 13, 840–855. https://doi.org/10.1038/nprot.2018.003.

Schmid, F., Wachsmuth, L., Schwalm, M., Prouvot, P.-H., Jubal, E.R., Fois, C., Pramanik, G., Zimmer, C., Faber, C., Stroh, A., 2016. Assessing sensory versus optogenetic network activation by combining (o)fMRI with optical Ca2+ recordings. J. Cereb. Blood Flow Metab.: Offc. J. Int. Soc. Cereb. Flow. Metabol. 36, 1885–1900. https://doi.org/10.1177/0271678X15619428.

Schölvinck, M.L., Maier, A., Ye, F.Q., Duyn, J.H., Leopold, D.A., 2010. Neural basis of global resting-state fMRI activity. Proc. Nat. Acad. Sci. U. S. A. 107, 10238–10243. https://doi.org/10.1073/pnas.0913110107.

Schulz, K., Sydekum, E., Krueppel, R., Engelbrecht, C.J., Schlegel, F., Schröter, A., Rudin, M., Helmchen, F., 2012. Simultaneous BOLD fMRI and fiber-optic calcium recording in rat neocortex. Nat. Methods 9, 597–602. https://doi.org/10.1038/nmeth.2013.

Schwalm, M., Schmid, F., Wachsmuth, L., Backhaus, H., Kronfeld, A., Aedo Jury, F., Prouvot, P.-H., Fois, C., Albers, F., van Alst, T., Faber, C., Stroh, A., 2017. Cortex-wide BOLD fMRI activity reflects locally-recorded slow oscillation-associated calcium waves. eLife 6. https://doi.org/10.7554/eLife.27602.

Sibson, N.R., Dhankhar, A., Mason, G.F., Rothman, D.L., Behar, K.L., Shulman, R.G., 1998. Stoichiometric coupling of brain glucose metabolism and glutamatergic neuronal activity. Proc. Natl. Acad. Sci. Unit. States Am. 95, 316–321. https://doi.org/10.1073/pnas.95.1.316.

Sinclair, M.D., 2003. A review of the physiological effects of alpha2-agonists related to the clinical use of medetomidine in small animal practice. Can. Vet. J. 44, 885–897.

Sinning, A., Hübner, C.A., 2013. Minireview: PH and synaptic transmission. FEBS Lett. 587, 1923–1928. https://doi.org/10.1016/j.febslet.2013.04.045.

Sommers, M., Pikkemaat, J., Booij, L., Heerschap, A., 2002. Improved anesthesia protocols for fMRI studies in rats: the use of medetomidine for stable, reversible sedation. Proc. Intl. Soc. Mag. Reson. Med. 10, 393.

Sun, Y.M., Favre, I., Schild, L., Moczydlowski, E., 1997. On the structural basis for size-selective permeation of organic cations through the voltage-gated sodium channel. Effect of alanine mutations at the DEKA locus on selectivity, inhibition by Ca2+ and H+, and molecular sieving. J. Gen. Physiol. 110, 693–715. https://doi.org/10.1085/jgp.110.6.693.

Talley, E.M., Solorzano, G., Lei, Q., Kim, D., Bayliss, D.A., 2001. Cns distribution of members of the two-pore-domain (KCNK) potassium channel family. J. Neurosci.: Offic. J. Soc. Neurosci 21, 7491–7505. https://doi.org/10.1523/JNEUROSCI.21-19-07491.2001.

Thompson, G.J., Merritt, M.D., Pan, W.-J., Magnuson, M.E., Grooms, J.K., Jaeger, D., Keilholz, S.D., 2013. Neural correlates of time-varying functional connectivity in the rat. Neuroimage 83, 826–836. https://doi.org/10.1016/j.neuroimage.2013.07.036.

Tian, R., Vogel, P., Lassen, N.A., Mulvany, M.J., Andreasen, F., Aalkjaer, C., 1995. Role of extracellular and intracellular acidosis for hypercapnia-induced inhibition of tension of isolated rat cerebral arteries. Circ. Res. 76, 269–275.

Tombaugh, G.C., Somjen, G.G., 1996. Effects of extracellular pH on voltage-gated Na+, K+ and Ca2+ currents in isolated rat CA1 neurons. J. Physiol 493 (Pt 3), 719–732. https://doi.org/10.1113/jphysiol.1996.sp021417.

van Hulzen, Z.J., Coenen, A.M., 1984. Photically evoked potentials in the visual cortex following paradoxical sleep deprivation in rats. Physiol. Behav. 32, 557–563. https://doi.org/10.1016/0031-9384(84)90309-3.

Vaucher, E., Tong, X.K., Cholet, N., Lantin, S., Hamel, E., 2000. GABA neurons provide a rich input to microvessels but not nitric oxide neurons in the rat cerebral cortex: a means for direct regulation of local cerebral blood flow. J. Comp. Neurol. 421, 161–171.

Vazey, E.M., Aston-Jones, G., 2014. Designer receptor manipulations reveal a role of the locus coeruleus noradrenergic system in isoflurane general anesthesia. Proc. Nat. Acad. Sci. U. S. A. 111, 3859–3864. https://doi.org/10.1073/pnas.1310025111.

Weber, R., Ramos-Cabrer, P., Wiedermann, D., van Camp, N., Hoehn, M., 2006. A fully noninvasive and robust experimental protocol for longitudinal fMRI studies in the rat. Neuroimage 29, 1303–1310. https://doi.org/10.1016/j.neuroimage.2005.08.028.

Westphalen, R.I., Hemmings, H.C., 2003. Selective depression by general anesthetics of glutamate versus GABA release from isolated cortical nerve terminals. J. Pharmacol. Exp. Ther. 304, 1188–1196. https://doi.org/10.1124/jpet.102.044685.

Williams, K.A., Magnuson, M., Majeed, W., LaConte, S.M., Peltier, S.J., Hu, X., Keilholz, S.D., 2010. Comparison of alpha-chloralose, medetomidine and isoflurane anesthesia for functional connectivity mapping in the rat. Magnet. Reson. Imag. 28, 995–1003. https://doi.org/10.1016/j.mri.2010.03.007.

Williams, R.H., Jensen, L.T., Verkhratsky, A., Fugger, L., Burdakov, D., 2007. Control of hypothalamic orexin neurons by acid and CO2. Proc. Natl. Acad. Sci. Unit. States Am. 104, 10685–10690. https://doi.org/10.1073/pnas.0702676104.

Zhao, F., Welsh, D., Williams, M., Coimbra, A., Urban, M.O., Hargreaves, R., Evelhoch, J., Williams, D.S., 2012. fMRI of pain processing in the brain: a within-animal comparative study of BOLD vs. CBV and noxious electrical vs. noxious mechanical stimulation in rat. Neuroimage 59, 1168–1179. https://doi.org/10.1016/j.neuroimage.2011.08.002.

Zhao, F., Zhao, T., Zhou, L., Wu, Q., Hu, X., 2008. BOLD study of stimulation-induced neural activity and resting-state connectivity in medetomidine-sedated rat. Neuroimage 39, 248–260. https://doi.org/10.1016/j.neuroimage.2007.07.063.

Zhurakovskaya, E., Paasonen, J., Shatillo, A., Lipponen, A., Salo, R., Aliev, R., Tanila, H., Gröhn, O., 2016. Global functional connectivity differences between sleep-like states in urethane anesthetized rats measured by fMRI. PLoS One 11. https://doi.org/10.1371/journal.pone.0155343 e0155343.